

Interaction of Spin-Labeled Lipid Membranes with Transition Metal Ions

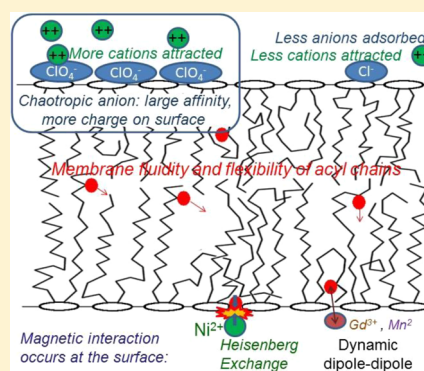
Boris Dzikovski,^{*,†,‡} Vsevolod Livshits,[‡] and Jack Freed^{*,†}

[†]National Biomedical Center for Advanced ESR Technology (ACERT), Department of Chemistry and Chemical Biology, Baker Laboratory, Cornell University, Ithaca, New York 14853, United States

[‡]Centre of Photochemistry, Russian Academy of Sciences, ul. Novatorov 7a, 117427 Moscow, Russia

Supporting Information

ABSTRACT: The large values of spin relaxation enhancement (RE) for PC spin-labels in the phospholipid membrane induced by paramagnetic metal salts dissolved in the aqueous phase can be explained by Heisenberg spin exchange due to conformational fluctuations of the nitroxide group as a result of membrane fluidity, flexibility of lipid chains, and, possibly, amphiphilic nature of the nitroxide label. Whether the magnetic interaction occurs predominantly via Heisenberg spin exchange (Ni) or by the dipole–dipole (Gd) mechanism, it is essential for the paramagnetic ion to get into close proximity to the nitroxide moiety for efficient RE. For different salts of Ni the RE in phosphatidylcholine membranes follows the anionic Hofmeister series and reflects anion adsorption followed by anion-driven attraction of paramagnetic cations on the choline groups. This adsorption is higher for chaotropic ions, e.g., perchlorate. (A chaotropic agent is a molecule in water solution that can disrupt the hydrogen bonding network between water molecules.) However, there is no anionic dependence of RE for model membranes made from negatively charged lipids devoid of choline groups. We used Ni-induced RE to study the thermodynamics and electrostatics of ion/membrane interactions. We also studied the effect of membrane composition and the phase state on the RE values. In membranes with cholesterol a significant difference is observed between PC labels with nitroxide tethers long enough vs not long enough to reach deep into the membrane hydrophobic core behind the area of fused cholesterol rings. This study indicates one must be cautious in interpreting data obtained by PC labels in fluid membranes in terms of probing membrane properties at different immersion depths when it can be affected by paramagnetic species at the membrane surface.



INTRODUCTION

Many biological processes involve interactions of ions with lipid membranes. A number of studies have focused on permeability and diffusion of small nonelectrolyte molecules (including water and oxygen) in lipid membranes as well as on the interaction of univalent ions and divalent calcium and magnesium^{1–3} with the membrane. Divalent transition metal cations are known to affect a number of cytoplasmic and membrane proteins.^{4,5} However, except for univalent ions and Ca²⁺ and Mg²⁺, only limited data are available on the interaction of metal ions with lipid membranes.^{3,6,7}

It has long been known that various inorganic and organic anions can affect membrane-related physiological processes. Nitrate and other anions can cause an increase in the twitch tension in muscle and muscle fibers,⁸ reversibly shift the voltage dependence of sodium and chloride channels of skeletal muscle,^{9,10} and affect the kinetics of Na, K-ATPase.^{11,12} The order of anionic effectiveness is often consistent with the so-called Hofmeister or lyotropic series, which originates from ranking the various ions with respect to their ability to precipitate chicken egg white proteins¹³ and correlates with their ability to disrupt the hydrogen bonding network between water molecules. Anionic effects obeying a similar order have

since been discovered for many membrane systems,^{9,10,14} including association constants to simple lipid bilayers.¹⁵ A typical Hofmeister series, in the order of the increasing chaotropic effect, is SO₄²⁻ < acetate < Cl⁻ < NO₃⁻ < I⁻ < ClO₄⁻ < SCN⁻.

Because lipid membranes are heterogeneous along the membrane normal, the effect of ions on membrane-embedded compounds should depend on the depth in the membrane. Such information for paramagnetic species can be provided by ESR using phospholipid spin-labels having a nitroxide moiety covalently attached to different positions in the acyl chain¹⁶ or other spin-labeled membrane-spanning compounds, such as WALP peptides,¹⁷ which have been suggested as rulers for studying membrane properties at different immersion depths. If the paramagnetic relaxation enhancement (RE) of these compounds is dominated by collisional spin exchange with paramagnetic molecules penetrating the membrane, like oxygen, the RE value is a direct measure of the product of local concentration and diffusion coefficient of the paramagnetic relaxant.^{2,18}

Received: August 22, 2015

Published: October 13, 2015

Previously, values of RE induced by several paramagnetic transition ion salts (perchlorates, chlorides, sulfates of nickel, copper, manganese, etc.) were measured for lipid spin-labels (*n*-PC) having doxyl groups in various positions of the acyl chain in the DMPC membrane.¹⁹ It was suggested that for nickel salts the spin–lattice RE of PC spin-labels in membranes is dominated by Heisenberg spin exchange between Ni²⁺ ions and spin-labels. However, how and where this exchange occurs remained unclear: the hypothesis offered that the large exchange rates were due to penetration of ions into the membrane.¹⁹ But this requires unrealistically high concentrations of ions in the hydrophobic core and/or some alternative non-Brownian diffusion mechanism (see discussion in Supporting Information, subsection 4).

In order to better understand the interaction of ionic compounds with membrane constituents, we study in the present work the RE for *n*-PC (*n* = 5, 7, 10, 12, 14, and 16) and DPPTC lipid spin-labels induced by various Ni²⁺ salts in model phospholipid membranes. It provided insight into the nature of the anionic dependence for the RE. Also, these data in comparison with those from other paramagnetic salts (e.g., Gd³⁺) provide better understanding of how and where the magnetic interaction between water-soluble paramagnetic salts and membrane-embedded nitroxide occurs. The results are discussed in terms of electrostatics, membrane fluidity, and flexibility of lipid molecules.

Our specific findings are the following:

1. The large values of relaxation enhancement (RE) for PC spin-labels in the phospholipid membrane induced by paramagnetic metal salts dissolved in the water phase can be explained by vertical fluctuations of nitroxide group due to membrane fluidity and flexibility of lipid chains. These fluctuations bring the nitroxide into close proximity with the ions near the membrane surface, and then the mechanism of magnetic interaction is either Heisenberg spin exchange (e.g., Ni²⁺, Cu²⁺), dipole–dipole interaction (Gd³⁺), or a combination of both (Mn²⁺).

2. The dependence of RE in phosphatidylcholine membranes on the counterion follows the anionic Hofmeister series. This dependence is explained by adsorption of anions onto choline groups since it does not exist for the negatively charged lipid (DMPG) devoid of the choline group. The value of the RE also depends on the presence of other ionic compounds in the water phase. The anion adsorption leads to attraction of cations to the membrane surface where their interaction with nitroxides occurs. These effects (e.g., for perchlorate) can be successfully simulated by solving the Poisson–Boltzmann–Graham equation, provided one takes into account the specific binding of perchlorate ions to choline groups and nickel ions to phosphates.

3. In a membrane with cholesterol, consistent with previous observations from frozen membranes,²⁰ a significant difference is observed between PC labels with nitroxide tethers long enough vs not long enough from the polar head to reach deep into the membrane hydrophobic core beyond the area of fused cholesterol rings.

4. The dipolar mechanism of paramagnetic relaxation between nitroxides and ions resulting from the relative diffusive motion of ions and nitroxides (Gd³⁺, Mn²⁺), manifests itself in (1) a more gradual slope of the RE on the spin-labeling position and (2) larger values of the T_2^{-1} RE vs the T_1^{-1} RE compared to the dominant Heisenberg exchange mechanism for Ni²⁺. This interaction is relatively long-range and can reach

the hydrophobic core of the membrane as suggested by our experiments using spin-labeled WALP, a rigid α -helical peptide spanning the membrane bilayer (Supporting Information, subsection 6).

5. We have recently shown that in frozen membranes PC spin-labels do not simply reflect the polarity gradient or water penetration profile.^{20,21} Instead, their ESR parameters reflect a complex equilibrium of hydrogen-bonded and non-hydrogen-bonded forms of nitroxide resulting from the flexibility of nitroxide tethers and existence of their U-shaped conformations; see also ref 22. This current work shows that similar caution should be taken when interpreting information obtained by PC labels in fluid membranes in terms of probing membrane properties at different immersion depths, in particular if the property studied can be substantially affected by paramagnetic ions at the membrane surface.

MATERIALS AND METHODS

Materials. Spin-labeled phosphatidylcholines, *n*-PC spin-labels (1-acyl-2-[*n*-(4,4-dimethylloxazolidine-*N*-oxyl)stearoyl]-*sn*-glycero-3-phosphocholine), were purchased at Avanti Polar lipids or synthesized as ref 16 from corresponding doxyl-stearic acids. Synthetic phosphatidylcholine, DMPC (1,2-dimyristoyl-*sn*-glycero-3-phosphocholine), and cholesterol were from Avanti Polar Lipids (Alabaster, AL). The paramagnetic salts were from Sigma (St. Louis, MO), Fluka (Buchs, Switzerland), and Merck (Germany). Methanol and chloroform were of analytical grade.

Preparation of Membrane Samples. Spin-labeled phosphatidylcholines were incorporated in bilayer membranes of DMPC at a relative concentration of 0.5 mol % by drying down the lipid solutions in chloroform/methanol and then suspending the dry lipid in water or appropriate salt solution above the chain melt temperature for at least 10 min. Since Ni²⁺ is slightly acidic, the solutions of its salts were typically at pH \approx 4. All membrane dispersions were prepared under argon from argon-saturated solutions. Aliquots of the dispersions containing 1 mg of the lipid were transferred into 50 μ L, 0.7 mm i.d. glass capillaries and spun down for 10 min at 10000g. The centrifuge was supplied with a capillary (microhematocrit) rotor. Sometimes, at high salt concentrations (\sim 1 M), the lipid pellet floats in the capillary instead of sinking. In this case most of the clear supernatant was removed from the capillary except approximately the volume of the pellet which was then resuspended in the remaining supernatant and used in ESR measurements.

To remove the remaining oxygen from the lipid and ensure anaerobic conditions in final ESR samples, the lipid pellet was then subjected to a triple freeze–thaw–pump deoxygenation cycle and sealed under slightly reduced argon pressure. If needed, sample sizes were trimmed to <5 mm length to avoid inhomogeneities in B_1 and B_m fields.²³

ESR Spectroscopy. ESR spectra were recorded at a microwave frequency of 9.4 GHz on a Bruker EMX or a BRUKER ELEXYS-II E500 spectrometer equipped with a nitrogen gas flow temperature unit. Sample capillaries were positioned along the symmetry axis of the standard 4 mm quartz ESR sample tube that contained dodecane for thermal stability. For saturation measurements samples were centered in the BRUKER Super High Q cylindrical cavity, and all spectra were recorded under critical coupling conditions. The heating of the sample owing to the effect of the microwave field was compensated by gradually adjusting the settings of the

temperature unit in the range of microwave power 4–0 dB. The correction at 0 dB was $\sim 4\text{--}5\text{ }^\circ\text{C}$ in the Super High Q cavity for the BRUKER ELEXYS-II E500 spectrometer. The estimate was obtained using control nonsaturating samples of vanadyl sulfate in water/glycerol with a strong dependence of the ESR spectrum on temperature. The volume of the control sample was chosen to match the dielectric losses in the standard membrane sample. The root-mean-square microwave magnetic field $(B_1^2)^{1/2}$ measurement for a “point” sample of aqueous peroxyamine disulfonate with known T_1 and T_2 ²⁴ gave 0.97 G. For lipid samples corrections were made for the cavity Q value as described in ref 23.

RESULTS

In this section we describe our experimental approach to the determination of RE for membrane-embedded spin-labels by paramagnetic ions (with main focus on Ni^{2+}). It includes saturation experiments and/or direct measurements of additional Lorentzian line broadening of unsaturated spectra. Using this approach, we study the counterion (i.e., the anion of the nickel salt) effect on the RE induced by Ni^{2+} and show that it follows the Hofmeister series for anions. We explain this Hofmeister type dependence by specific adsorption of anions on the choline groups followed by attraction of Ni^{2+} ions to the emerging net negative charge of the membrane surface. This is supported by experiments in DMPG vs DMPC and by studying the RE dependence on the concentration of different nickel salts as well as on the addition of nonparamagnetic electrolytes. A model based on the Poisson–Boltzmann–Graham equation taking into account the specific binding of Ni^{2+} ions to phosphate groups and anions to choline groups provides good quantitative agreement with experiment. In this part we also discuss the effects of cholesterol and of the phase state of the membrane.

1. Microwave Saturation Studies of Paramagnetic Ni^{2+} -Induced RE Depends on Counterions and Depth of Position in the Membrane. The standard CW progressive saturation method of determining spin–lattice RE of spin-labels in membranes is described in refs 25–28. In the present work we follow that approach such that the dependence on the microwave field strength of the amplitude of the central component of the ESR spectrum I is given by the equation

$$I = \frac{I_0 B_1}{(1 + P B_1^2)^\epsilon} \quad (1)$$

where the saturation parameter $P = \gamma^2 T_1 T_2^{\text{eff}}$. T_2^{eff} takes into account intrinsic homogeneous and motion-induced transverse relaxation (also homogeneous), and the exponent ϵ is an empirical correction factor. $\epsilon = 1.5$ for homogeneous and $\epsilon \sim 0.5$ for inhomogeneous broadening.²⁸ Thus, P and ϵ are determined from measuring the amplitude of the ESR signal vs microwave magnetic field strength, B_1 , and following fitting procedures. The efficiency of a paramagnetic compound in inducing RE then was determined as $\Delta(1/P) = 1/P_{\text{ion}} - 1/P_0$, where P_{ion} and P_0 are respectively the values of the saturation factor in the presence/absence of paramagnetic relaxant, respectively.

This is a simple and convenient method that has proved sufficient for this and previous related studies when compared to line width measurements because it allows the detection of weaker RE, since T_1 for nitroxides in the systems studied is more than order of magnitude longer than T_2 and usually more

sensitive to weak magnetic interactions with other paramagnetic compounds. The more rigorous approach would be to simulate and fit spectra with the theory for slow motion in the presence of ESR saturation for direct determination of T_1 (cf. ref 29), but this awaits a more modern version of simulation software along the lines of^{30,31} current theory for unsaturated spectra to be useful. Simplified versions were developed for simulations of saturated spectra in refs 32 and 33. They used two molecular models: rapid rotational diffusion or strong-jump diffusion of unrestricted frequency within a cone of fixed maximum amplitude. It has been shown¹⁹ that within accuracy of these models the nitroxide RE caused by Ni^{2+} salts for membrane-embedded spin-labels satisfies the condition $\Delta T_2^{-1} \approx \Delta T_1^{-1}$, while Mn^{2+} ions induce $\Delta T_2^{-1} > \Delta T_1^{-1}$.

Typical saturation curves for cases corresponding to different P values are shown in Figure 1. The dependence of saturation

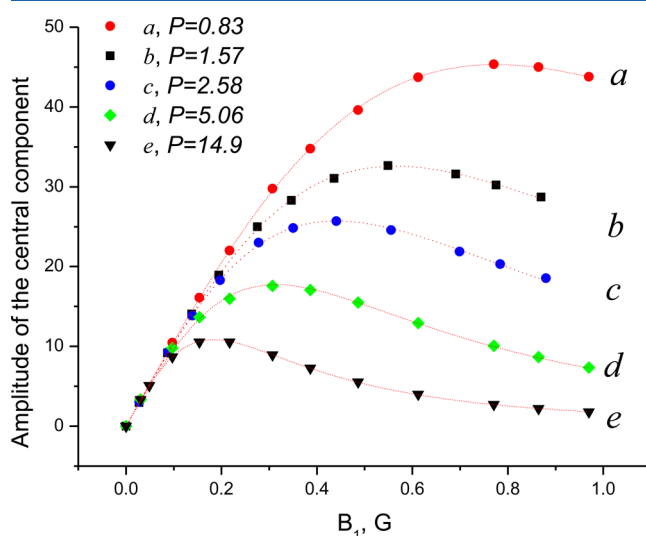


Figure 1. Examples of experimental saturation curves in fully hydrated deoxygenated DMPC membranes corresponding to different values of the saturation factor $P = \gamma^2 T_1 T_2^{\text{eff}}$. (a) 5-PC, 10 mM nickel perchlorate, $P = 0.83\text{ G}^{-2}$; (b) 10-PC, 30 mM nickel nitrate, $P = 1.57\text{ G}^{-2}$; (c) 12-PC, 30 mM nickel chloride, $P = 2.58\text{ G}^{-2}$; (d) 16-PC, 30 mM nickel sulfate, $P = 5.06\text{ G}^{-2}$; (e) 16-PC, water with no ions, $P = 14.91\text{ G}^{-2}$. Red lines are fits of the experimental data to eq 1. $T = 39\text{ }^\circ\text{C}$.

parameters on the PC label position in the presence or absence of paramagnetic relaxant in DMPC membranes is shown in Figure 2. Figure 3 shows the efficiency of RE, $\Delta(1/P)$ for different salts of Ni depending on the PC labeling position. Note that the data are shown for 30 mM of each nickel salt, except the most efficient relaxation agent among them, $\text{Ni}(\text{ClO}_4)_2$, which is used at 10 mM concentration.

2. Relaxation Broadening of the Low-Power ESR Spectra. The relaxation enhancement is also manifested in the broadening of the low-power unsaturated ESR spectra. We found that in all cases this additional broadening could be well described by a Lorentzian line shape, and the ESR line in the presence of relatively low concentrations of Ni^{2+} ions could be fit well to the convolution of the initial line shape in the absence of Ni^{2+} ions with an appropriate Lorentzian line (Figure 4a).

Although ESR spectra in the presence of low concentration Ni^{2+} salts can be simulated satisfactorily by convolution of the initial ESR spectrum (in the absence of Ni^{2+}) with the corresponding Lorentzian function (Figure 4a), at larger Ni^{2+}

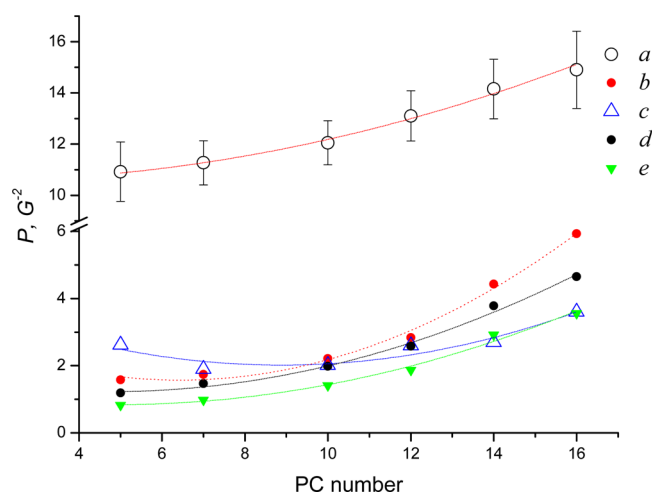


Figure 2. Profiles of the saturation factor $P = \gamma^2 T_1 T_2^{\text{eff}}$ in DMPC membrane for different relaxants vs PC number. P was determined from saturation curves for a series of phospholipids systematically labeled at the *sn*-2 acyl chain at positions $n = 5, 7, 10, 12, 14,$ and 16 . (a) No relaxant, oxygen is removed; (b) 30 mM nickel sulfate added, no oxygen; (c) air oxygen, samples are prepared in aerobic conditions; (d) 30 mM nickel chloride, no oxygen; (e) 10 mM nickel perchlorate, no oxygen. $T = 39^\circ\text{C}$.

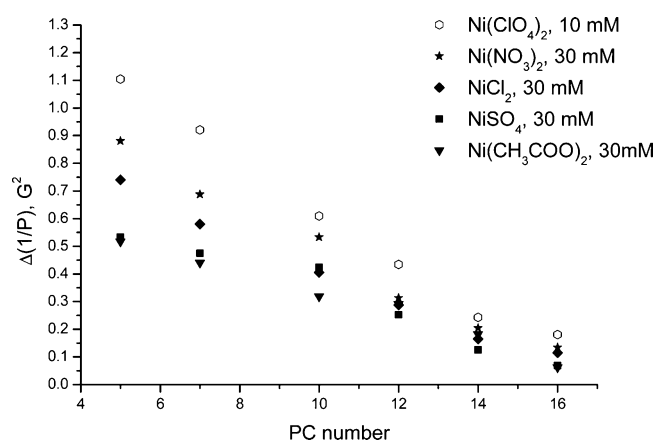


Figure 3. Efficiency of different nickel salts in inducing RE in 5, 7, 10, 12, 14, and 16 PC spin-labels in DMPC membrane at 39°C , measured as $\Delta(1/P) = 1/P_{\text{ion}} - 1/P_0$, where P_{ion} and P_0 are the values of the saturation factor P in the presence and absence of relaxant.

concentrations such a convolution of the “zero nickel” spectrum did not give a good fit, with the discrepancy progressively increasing with Ni concentration. These spectral changes are indicative of ion binding affecting the membrane structure and dynamics by causing partial immobilization of spin-labels. We found that the spectra at high concentrations of Ni salts can best be simulated if the spectrum of the same concentration of a corresponding Mg^{2+} salt is taken as the starting point for convolution.

In the same fashion, 10 mM of $\text{Cu}(\text{ClO}_4)_2$ in the aqueous phase causes changes in the ESR line shape for 5, 7, and 10 PC's which cannot be approximated with a Lorentzian broadening of the initial spectrum. The nonmagnetic effect of Cu^{2+} is rather similar to the effect of Ca^{2+} , so the spectra in the presence of $\text{Cu}(\text{ClO}_4)_2$, for example, can be successfully simulated by introducing additional Lorentzian broadening to the corresponding spectra in the presence of 10 mM

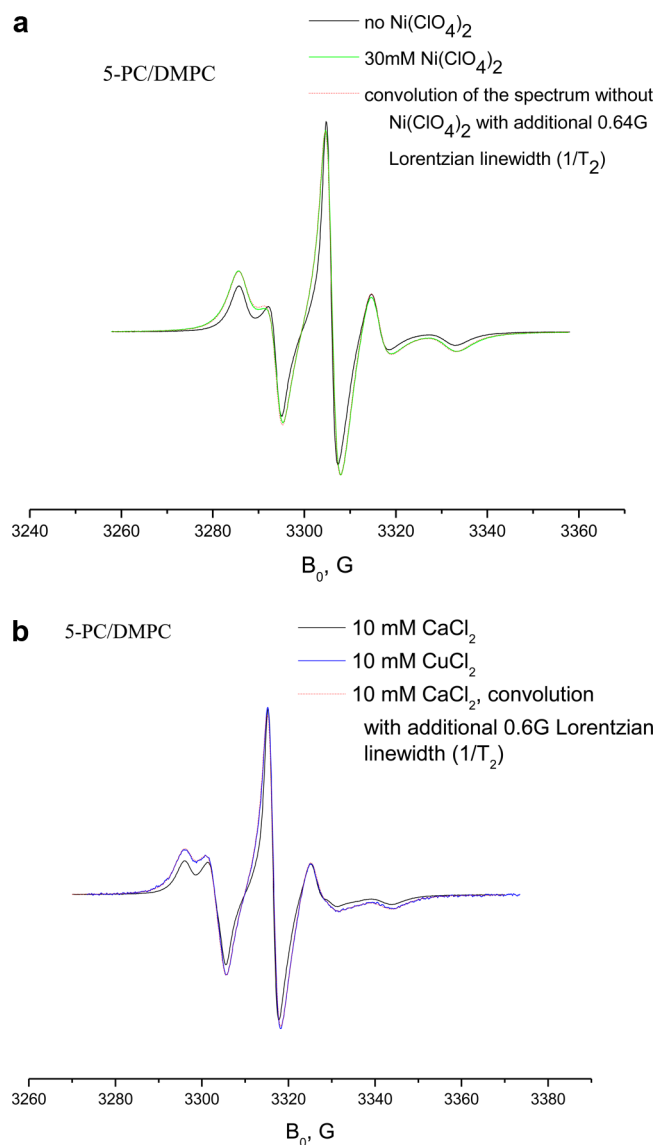


Figure 4. (a) ESR spectrum of 5-PC in the presence of $\text{Ni}(\text{ClO}_4)_2$ can be derived by convolution of a spectrum in the absence of $\text{Ni}(\text{ClO}_4)_2$ with the Lorentzian function. Spectrum in the absence of $\text{Ni}(\text{ClO}_4)_2$ (blue); spectrum in the presence of 30 mM $\text{Ni}(\text{ClO}_4)_2$ (green); convolution of the spectrum in the absence of $\text{Ni}(\text{ClO}_4)_2$ with additional 0.64 G ($1/T_2$) Lorentzian line width (red). (b) ESR spectrum of 5-PC in the presence of $\text{Cu}(\text{ClO}_4)_2$ can be derived by convolution of a spectrum in the presence of $\text{Ca}(\text{ClO}_4)_2$ with the Lorentzian function. Spectrum in the presence of 10 mM of $\text{Ca}(\text{ClO}_4)_2$ (black); spectrum in the presence of 10 mM $\text{Cu}(\text{ClO}_4)_2$ (blue); convolution of the spectrum in the presence of $\text{Ca}(\text{ClO}_4)_2$ with additional 0.6 G ($1/T_2$) Lorentzian line width (red).

$\text{Ca}(\text{ClO}_4)_2$. (Figure 4b). Similarly, to estimate the broadening effect of Gd^{3+} ions on PC spin-labels, we used spectra with the corresponding La^{3+} salt as the starting point for the convolution.

Although literature data on binding constants to phospholipid membranes for different ions is very divergent, these observations indicate similar nonmagnetic effects of Ni^{2+} and Mg^{2+} on the membrane structure and likely similar specific affinity for phosphate groups. These results are consistent with our DSC data (Supporting Information, subsection 1) which show little difference between Ni^{2+} and Mg^{2+} salts in their

effects on the main chain-melting transition and the L_{β} - P_{β} pretransition for DMPC. Similar comparative behavior is observed for Ca^{2+} and Cu^{2+} salts

3. Relaxation Enhancement of PC Spin-Labels by Different Nickel Salts. The order of relaxation enhancement, for both $\Delta(1/P)$ and relaxation broadening, by different Ni^{2+} salts (Figures 3 and 5) as well as by Cu^{2+} salts (Supporting

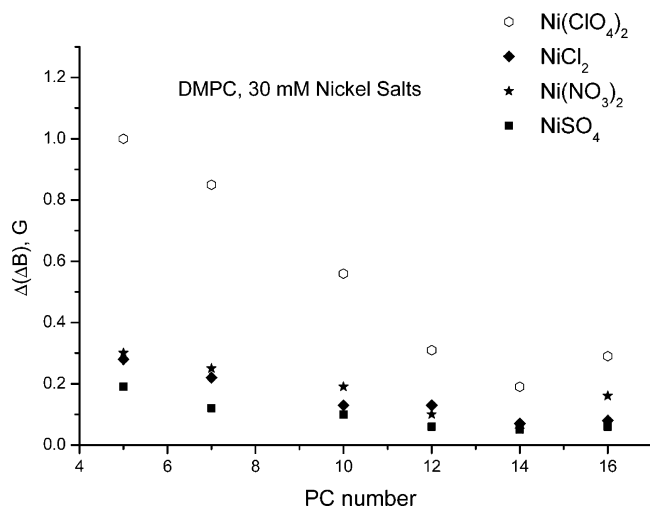


Figure 5. Broadening of the central spectral component due to T_2 relaxation enhancement by different nickel salts at 30 mM concentration in the series of PC spin-labels.

Information, subsection 2) is in good agreement with the Hofmeister series. Also, the magnitude of the RE for all Ni^{2+} salts decreases monotonically with an increase in distance of the labeling position from the PC polar head.

4. Spin-Label Relaxation Enhancement in DMPG Membranes. As shown above, the effect of anions on the RE in DMPC membranes follows the anionic Hofmeister series. This anion dependence of RE can be due, in principle, to anion adsorption on choline groups of PC resulting in the anion driven attraction of Ni^{2+} ions to membrane surface. Thus, the association constants for iodide, thiocyanate, and perchlorate for neutral POPC membranes increase in the order expected for the Hofmeister series of anions.¹⁵ Alternatively, the effect of anions on the RE could be due to partition of Ni^{2+} ions associated with anions in ion pairs into the lipid membrane.

To explore this effect further, we also studied DMPG membrane. DMPG is a negatively charged lipid devoid of a choline group. The pK_a of DMPG is reported to be³⁴ 2.9, indicating that in our experimental conditions, $\text{pH} \sim 4$ for 10 mM nickel in water, it is negatively charged. If the difference in RE between chloride and perchlorate in DMPC is caused by different binding of anions to cholines followed by electrostatic attraction of cations, we would expect little anion dependence of the RE in DMPG, since there is no choline and the headgroup has a net negative charge directly binding the cations. In a sense then, the DMPG experiment can be considered an important test. An absence of anion dependence for RE in DMPG would indicate that the anion effect in DMPC is not due to partition of ion pairs into the membrane as was suggested in ref 19 but to an anion-driven increase in the surface concentration of Ni^{2+} ions.

However, to relate the broadening results in DMPC vs DMPG, one has to be sure that DMPG at the experimental conditions forms a bilayer. At low ionic strength hydrated DMPG exists in a nonbilayer form.³⁵ Water–DMPG mixtures do not pellet and do not look like a suspension but rather like a transparent viscous gel. Once the ionic strength is increased sufficiently to achieve complete screening of the headgroup charge by Na^+ ions, DMPG forms a bilayer and behaves very similar to DMPC.³⁵ ESR and DSC experiments showing the main lipid phase transition at 24.4 °C, as well as simple visual inspection, clearly indicate that in the presence of 10 mM of Mg^{2+} or Ni^{2+} salts DMPG forms a bilayer for our experimental conditions. We then determined the line width values for 5-, 7-, and 14-PC in fluid DMPG membrane for the same nickel salts in the presence of 2 M NaCl. The DMPG/2 M NaCl has previously been used as a reference for the bilayer state of DMPG.³⁶

The difference in the magnitude of RE in the presence/absence of 2 M NaCl can be quantitatively described in electrostatic terms. The absolute values of Ni^{2+} induced line width for DMPG in the absence of additional NaCl are considerably higher compared with the DMPC membranes. A significant result, however, is that as seen in Figures 6 and 7, the line width in a DMPG bilayer shows little anion effect. This supports the conclusion that adsorption of anions on choline groups of phospholipids causes the observed anion dependence of RE for DMPC membranes.

5. Adsorption of Nickel Ions on the Membrane Surface. Estimates from the Ni^{2+} Depletion of the Water Phase. The anion-driven adsorption of cations on the membrane interface could be estimated from the concentration of nickel ions in the aqueous phase of the membrane compared to their total added concentration. For this purpose a membrane suspension prepared with known total concentrations of $\text{Ni}(\text{ClO}_4)_2$ of 10 or 30 mM with 0.2 mM of a water-soluble spin probe was spun down after mild sonication. The concentration of Ni^{2+} ions in the supernatant was estimated from the nitroxide ESR line width. The lipid pellet consists of the lipid multilayer, and the remaining ions are assumed to be located in the aqueous subphase of the multilayer. 100 mg/mL lipid suspensions (147 mM lipid suspended in the water phase) showed a concentration of 5.2 mM Ni^{2+} in the water phase for suspensions prepared with 10 mM $\text{Ni}(\text{ClO}_4)_2$ and 20.4 mM for 30 mM $\text{Ni}(\text{ClO}_4)_2$. Two water-soluble spin-labels, TEMPOL and PD-Tempone, gave the same result. They yield ~ 4.8 and ~ 9.6 mM, respectively, of nickel ions associated with corresponding “binding constants” of 6.3 and 3.2 M^{-1} . It illustrates that the adsorption cannot be described by a simple Langmuir isotherm as we will discuss below.

This nickel depletion experiment on DMPG membranes showed that all added Ni^{2+} is adsorbed at the membrane surface, with no measurable broadening for spin-labels in the supernatant until the DMPG/ Ni ratio reaches 2:1. Then the aqueous concentration of Ni^{2+} grows linearly with added nickel salt. This suggests that a 2:1 ratio corresponds to full surface coverage for DMPC with one Ni^{2+} ion likely bound to two head groups.

Interestingly, the additional broadening of PC labels in DMPG upon addition of Ni^{2+} ions levels off before the Ni/DPPC ratio of 1:2, but here the result can be affected by changes in membrane dynamics/structure upon further addition of Ni^{2+} or Mg^{2+} ions (Figure 8b).

2 mg DMPG with 0.5% (mol.) of 5-PC + 50 μ l of 10mM salts:

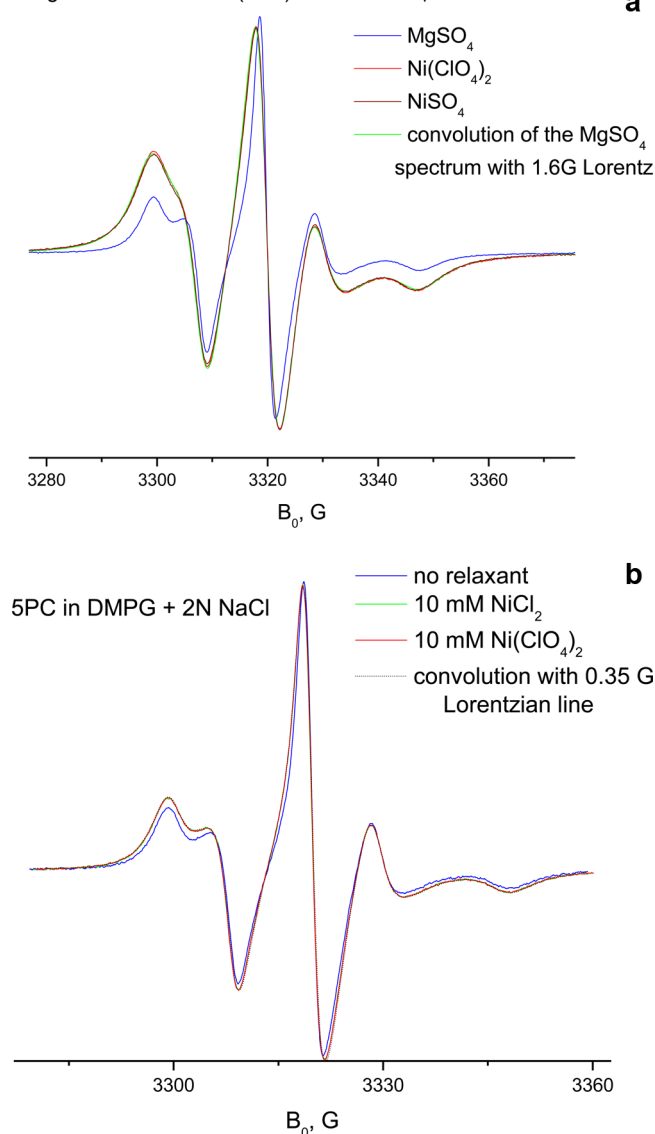


Figure 6. (a) Spectra of SPC in DMPG (0.5 mol %) hydrated with 10 mM solutions of MgSO_4 , NiSO_4 , or $\text{Ni}(\text{ClO}_4)_2$. (b) Spectra of SPC in DMPG (0.5 mol %) in the presence of 10 mM NiSO_4 or $\text{Ni}(\text{ClO}_4)_2$ and 2 M NaCl. (c) Broadening of different *n*-PC spin-labels in DMPG membranes without NaCl (see (a)) in the presence of 10 mM NiSO_4 or $\text{Ni}(\text{ClO}_4)_2$.

For comparison of Ni^{2+} and Gd^{3+} , the same depletion experiment with 10 mM of GdCl_3 instead of $\text{Ni}(\text{ClO}_4)_2$ gave 4.7 mM of GdCl_3 remaining in the water phase from 10 mM of initially added concentration. It yields an apparent binding constant of $\sim 8 \text{ M}^{-1}$ at these conditions and the surface concentration of Gd^{3+} from GdCl_3 similar to the surface concentration of Ni^{2+} from $\text{Ni}(\text{ClO}_4)_2$.

6. Effect of Metal Complexation on RE. Experiments on RE by complexing compounds provide more evidence that adsorption of paramagnetic ions on the membrane interface plays a critical role in their interaction with the nitroxide moieties of spin-labeled lipids. As seen in Figure 9, complex formation of Ni^{2+} ions with EDDA completely hinders their RE effects on membrane-embedded spin-labels. On the other hand, this Ni^{2+} –EDDA complex has almost the same effect as NiCl_2 or $\text{Ni}(\text{ClO}_4)_2$ on the line width of TEMPO interacting with

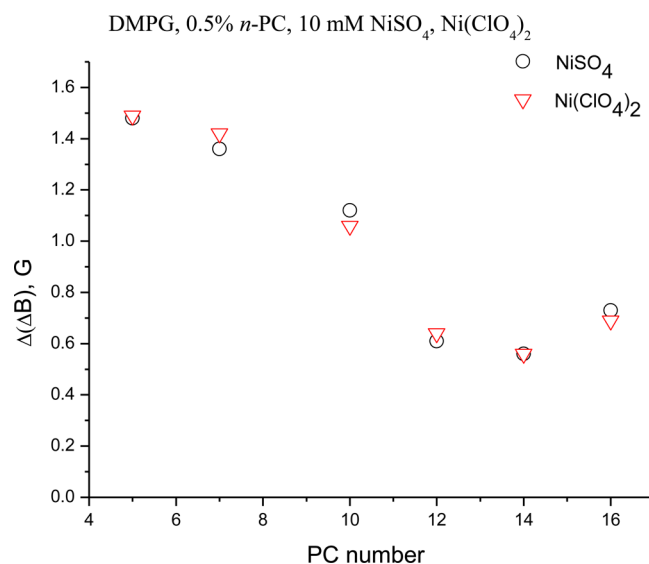


Figure 7. Broadening of different *n*-PC spin-labels in DMPG membranes without NaCl (see Figure 6a) in the presence of 10 mM NiSO_4 or $\text{Ni}(\text{ClO}_4)_2$.

them via Heisenberg exchange in water. Apparently, RE of spin-labeled lipids by Ni^{2+} is caused by nickel ions bound to the membrane, and preventing this binding by complex formation eliminates the RE. A similar total elimination of RE was observed upon complexation of Ni^{2+} ions by water-soluble crown ethers. Moreover, membrane-embedded spin-labels show little RE from potassium chromium oxalate (CROX), which is about twice as efficient a broadening agent in water than Ni^{2+} . Interestingly, another negatively charged complex ion, introduced as $\text{K}_3\text{Fe}(\text{CN})_6$, causes some measurable RE with $\Delta(1/P)$ for 10PC, for example, is $\sim 0.07 \text{ G}^2$ (see also ref 19) although its effect is weaker than for most paramagnetic cations studied. This may be explained by strong adsorption of $\text{Fe}(\text{CN})_6^{3-}$ ions on the choline group due to its high polarizability which should place this ion in the Hofmeister series near ClO_4^- (cf. ref 37).

7. Dependence of the Relaxation Enhancement on the Concentration of a Paramagnetic Ion. The dependence of RE on the concentration of nickel salts in the aqueous phase was studied for different phospholipid spin-labels (Figure 10). The relaxation enhancements were determined from the line width broadening ($\Delta\Delta B_0$) for several PC spin-labels in DMPC membranes in the presence of increasing concentrations of Ni perchlorate and chloride at 39 °C. The $\Delta\Delta B_0$ values were determined by convolution of the initial ESR spectrum in the absence of Ni^{2+} , but in the presence of the corresponding Mg^{2+} salt, with a Lorentzian function of variable width to achieve the best fit.

As seen in Figure 10, the concentration dependence of the RE tends to level off at high nickel salt concentration. This suggests that the RE is determined by adsorption of Ni^{2+} ions at the membrane surface, which approaches a limit with increasing concentration of Ni^{2+} in the water phase. This dependence is, however, substantially different from a simple Langmuir pattern and can be described by a model that accounts for the electrostatic interaction of adsorbed ions (see below).

8. Membrane Surface Potential and Nickel Adsorption in the Presence of Specific Adsorption of Anions and Cations. We explain the dependence of line broadening on the concentration of Ni perchlorate shown in Figure 10, as

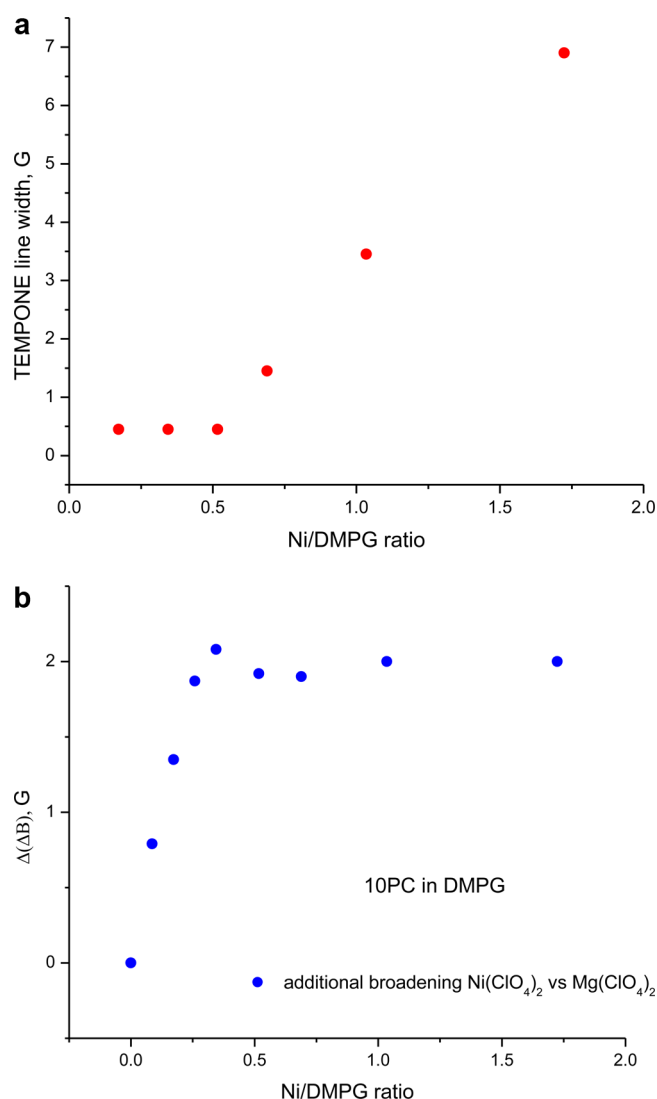


Figure 8. (a) Tempone line width in the supernatant obtained from DMPC hydrated by suspending in solutions of Ni(ClO₄)₂ of different concentration as a function of total Ni/DMPC ratio. (b) Broadening of 10PC/DMPC mixture hydrated by different concentrations of Ni(ClO₄)₂ depending on total Ni/DMPC ratio.

well as the larger values of RE by Ni(ClO₄)₂ compared to other nickel salts, by adsorption of perchlorate anions on choline groups followed by electrostatic attraction of paramagnetic cations to the emerging negative surface charge. To further explore the role of membrane electrostatics in attracting Ni²⁺ ions to the membrane surface, we also studied the changes in the line broadening of PC labels by 30 mM Ni(ClO₄)₂ in the presence of univalent electrolytes in the water phase: NaClO₄ with the anion capable of binding to the choline group of DMPC and the nearly indifferent electrolyte NaCl, since Cl⁻ ions have less affinity to cholines compared to ClO₄⁻.

Addition of an indifferent electrolyte should cause Debye screening of the negative surface charge, decrease in surface potential, and hence decrease in the concentration of nickel ions attracted to the membrane surface. For NaClO₄ this screening effect will compete with the initial increase in adsorption of perchlorate ions causing more negative charge and attracting more nickel ions. Indeed, as seen in Figure 11a, addition of NaCl to spin-labeled membrane in the presence of

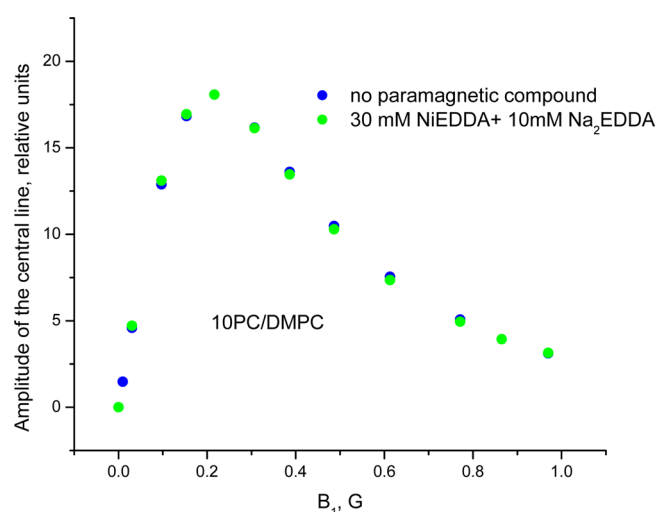


Figure 9. Saturation curves for 10PC/DMPC at 39 °C in the presence/absence of 30 mM of NiEDDA complex in the water phase.

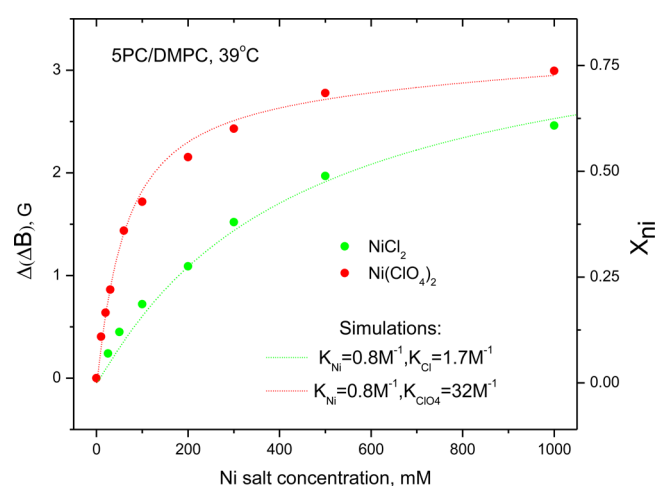


Figure 10. Dependence on the concentration of NiCl₂ and Ni(ClO₄)₂ in aqueous phase of the additional relaxation broadening of the EPR spectra of 5-PC in DMPC membranes at 39 °C. The dotted lines show simulations using the model described in the text (Results, subsection 8) with Ni:DMPC stoichiometry 1:2 and following values of binding constants: K_{Ni} = 0.8 M⁻¹, K_{Cl} = 1.7 M⁻¹, and K_{ClO₄} = 32 M⁻¹.

Ni(ClO₄)₂ causes a steady drop in the line broadening. On the other hand, upon addition of NaClO₄ the PC spin-label line width initially sharply increases, reaches a plateau, and then starts to drop slightly at higher concentrations (Figure 11b).

To show that our observations are consistent with anion-driven adsorption of cations and semiquantitatively simulate the experimental results, we applied the Poisson–Boltzmann–Graham equation.³⁸ The approach is similar to ref 15, but we also took into account specific binding of Ni ions to phosphate groups with a binding constant K_{Ni}. In the Poisson–Boltzmann–Graham equation

$$\sigma^2 = 2000\epsilon_0\epsilon_D RT \sum_i C_i^{\text{eq}} [e^{-z_i F_0 \Psi_0 / RT} - 1] \quad (2)$$

where ϵ_0 is the permittivity of free space, ϵ_D is the dielectric constant of water, T is the absolute temperature, R is the gas constant, C_i^{eq} is the concentration at equilibrium of ion i , having valence z_i , in the bulk aqueous phase, Ψ_0 is the electrostatic potential in the membrane plane, and F_0 is the Faraday

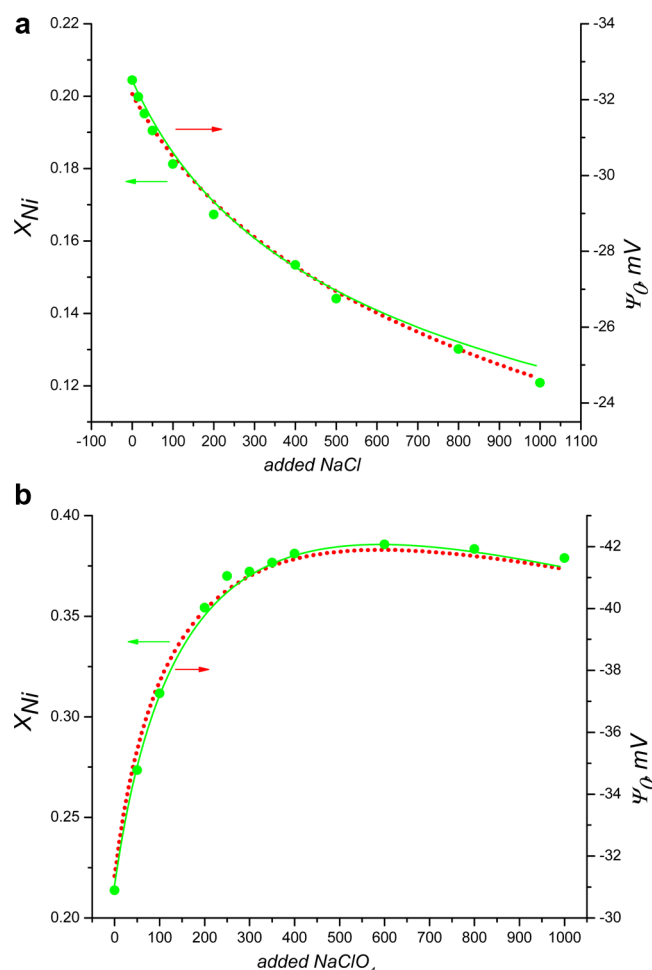


Figure 11. Dependences of the DMPC membrane surface coverage by Ni^{2+} ions on the concentration of NaCl and NaClO_4 in aqueous phase in the presence of 30 mM $\text{Ni}(\text{ClO}_4)_2$. $T = 39^\circ\text{C}$. The surface coverage X_{Ni} is calculated from line broadenings assuming 2:1 DMPC:Ni stoichiometry. (a) 10PC, addition of NaCl; (b) SPC, addition of NaClO_4 . Experimental data are shown by the small closed circles, and simulations for X_{Ni} based on the Graham–Poisson–Boltzmann model are shown by solid lines; simulations for Ψ_0 are shown by dotted lines. In these simulations the following values of binding constants are used: $K_{\text{Ni}} = 0.8$, $K_{\text{ClO}_4} = 32$, $K_{\text{Cl}} = 2$, and $K_{\text{Na}} = 0$.

constant. The summation is over all ions i (both anions and cations) in solution.

σ is the surface charge density on the membrane due to the adsorption of anions on cholines and/or cations on phosphates. The fractional coverage due to adsorption, X_i , is calculated using the modified Langmuir isotherm:

$$X_i = \frac{K_i C_i^M}{1 + K_i C_i^M + \sum_j K_j C_j^M} \quad (3)$$

where C_i^M is the concentration of the ions at the membrane surface, K_i its binding constant, and C_j^M and K_j are the surface concentrations and binding constants for other ions competing for the same binding site.

The membrane surface ion concentrations can be obtained from the concentrations in the bulk water phase using the Boltzmann relation:

$$C_i^M = C_i^{\text{eq}} e^{-z_i F_0 \Psi_0 / RT} \quad (4)$$

Finally, the surface charge density can be expressed as $\sigma = (-e/S) \sum_i z_i X_i$, which can be used in the left side of (2).

This procedure yields, for example, for a system containing Ni^{2+} and monovalent anions a ninth degree polynomial of $e^{F_0 \Psi_0 / RT}$. By numerically solving the equation and selecting appropriate roots the concentration of free Ni^{2+} ions in the diffuse layer at the membrane surface (C_{Niim}) and mole fraction X_{Ni} of phosphates bound to Ni^{2+} are calculated.

Our purpose was to simulate the shape of the experimental concentration dependences for the line broadening. To relate the line broadening values and X_{Ni} , we used our supernatant depletion experiments. Extrapolating these values to the condition of the experiments from Figures 10 and 11 yields estimates of the number of Ni molecules per headgroup as $\sim 0.095\text{--}0.105$ at 30 mM added $\text{Ni}(\text{ClO}_4)_2$, i.e., either $X_{\text{Ni}} \sim 0.1$ if one assumes full surface coverage of one nickel ion per one headgroup or $X_{\text{Ni}} \sim 0.2$ for 2:1 DMPC/ Ni^{2+} limiting ratio. The latter was observed for DMPC/ Ni^{2+} (cf. subsection 5) and which is the same as the POPC/ Ca^{2+} ratio determined by NMR and atomic adsorption spectroscopy.³⁹ In our simulations we also assumed that X_{Ni} values are proportional to the line width. We found reasonable fits of our experimental data for either DMPC/Ni stoichiometry. However, the binding constants obtained were sensible for the 2:1 stoichiometry ($K_{\text{Ni}} = 0.7\text{--}0.8 \text{ M}^{-1}$, $K_{\text{ClO}_4} \sim 30\text{--}32 \text{ M}^{-1}$, and $K_{\text{Cl}} \sim 1.5\text{--}2 \text{ M}^{-1}$) but not for the 1:1 case ($K_{\text{Ni}} = 0.2\text{--}0.3 \text{ M}^{-1}$, $K_{\text{ClO}_4} \sim 36\text{--}40 \text{ M}^{-1}$, and $K_{\text{Cl}} = 3\text{--}4 \text{ M}^{-1}$). Also, this analysis shows that sodium ions do not specifically adsorb on the membrane in our conditions.

The literature data on binding constants of anions and cations are extremely divergent, even if measured by the same method. The contradictions in the results on ion binding constants have been discussed repeatedly in the literature and attributed to different methods used and distinct experimental conditions.⁴⁰ Different authors give for the binding constant to PC vesicles values in the range of $70\text{--}220 \text{ M}^{-1}$ for ClO_4^- , $2\text{--}8 \text{ M}^{-1}$ for NO_3^- , $0\text{--}1.7 \text{ M}^{-1}$ for Cl^- , $0\text{--}0.5 \text{ M}^{-1}$ for Na^+ , etc.^{15,41,42} It is still discussed in the literature if Cl^- and Na^+ are binding to membranes at all, e.g., ref 43. The values obtained for divalent ions are even more divergent: for Ca^{2+} they are given in the range of $\sim 1\text{--}1000 \text{ M}^{-1}$, for Mg^{2+} $1\text{--}30 \text{ M}^{-1}$, etc.,^{40,44} by different studies. The K_{Ni} value obtained by McLaughlin et al.⁴⁵ from electrophoretic measurements on liposomes is 0.83 M^{-1} , but another study⁴⁶ gives a value of 7.5 M^{-1} . Moreover, the literature results on these constants may not quite apply to our system, which is substantially different from most studies on ion binding to membranes. We work with multilamellar vesicles at $\text{pH} \sim 4$ and higher lipid/ion ratios than in electrophoretic experiments. The lower pH might affect the binding constants, decreasing them for cations and slightly increasing them for weakly binding anions due to competition with either H^+ or OH^- . However, even without a discussion of the “correct values” of binding constants, our experiments shown in Figures 10 and 11 allow for several conclusions: (1) the DMPC/Ni stoichiometry is likely 2:1. Assuming 1:1 stoichiometry requires extremely low values for K_{Ni} with X_{Ni} never approaching 1/2, and it suggests a different chemical nature for Ni^{2+} binding to phosphates on PC and PG. (2) At our conditions Cl^- ion binds to the membrane, while Na^+ does not. Figures 3 and 5 also support this conclusion of noticeable Cl^- binding, placing Cl^- in the Hofmeister series near NO_3^- . (3) Although our value of K_{ClO_4} in DMPC is somewhat less

than its literature range, it exceeds the binding constant of any other ion in this study by more than an order of magnitude. One can see that the simulations using Poisson–Boltzmann–Graham equation give a reasonable quantitative description of our experimental results, illustrating that addition of a chaotropic anion causes strong anion-driven attraction of paramagnetic cations and explains the observed Hofmeister series effects. One can see from Figure 11 that upon addition of both NaCl and NaClO₄ the surface concentration of adsorbed Ni²⁺ ions approximately follows the electrostatic potential in the membrane plane.

9. Effect of Cholesterol. Figure 12 shows the broadening of the ESR center line for PC spin-labels by 30 mM Ni(ClO₄)₂

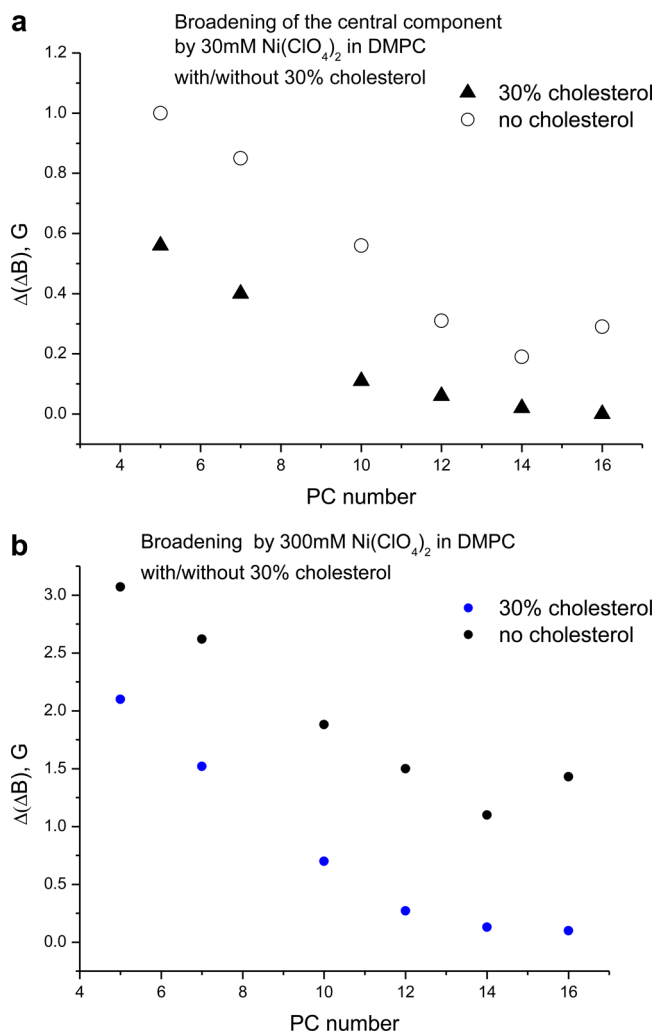


Figure 12. Broadening of PC labels spectra by Ni(ClO₄)₂ in membranes of DMPC or DMPC with 30 mol % cholesterol: (a) 30 mM and (b) 300 mM Ni(ClO₄)₂.

in a DMPC membrane containing 30 mol % cholesterol compared to DMPC membrane without cholesterol. One can see that in the presence of cholesterol there is hardly any broadening for PC spin-labels located on acyl chain positions that are typically in the membrane hydrophobic core below the area of the fused cholesterol rings ($n > 10$). This is in good agreement with polarity results recently obtained by low-temperature high-field ESR.²⁰ In frozen membranes containing cholesterol there is an abrupt decrease in the fraction of

hydrogen-bonded nitroxide for PC's $n \geq 10$. It was explained by the affinity of the nitroxides to locate in the extra free volume below the cholesterol rings, thereby greatly reducing their propensity to seek the membrane surface by taking on bent (U-shaped) conformations (cf. Discussion). This latter effect is observed at low temperature in frozen membranes where the dynamics of this process is frozen. As seen in Figure 12, the effect of cholesterol in the fluid membrane is similar. For $n > 10$, Ni(ClO₄)₂ induces little additional broadening, and positions 14 and 16 show no broadening effect even at very high relaxant concentration in the water phase. This result can be explained in terms of the extra free volume available for the nitroxides located beyond cholesterol rings and also by the barrier provided by cholesterol, which prevents the radical moieties from reaching the membrane surface from the interior.

10. Phase State of the Membrane. In the study of the behavior of PC spin-labels in the gel phase of phospholipid membranes with or without cholesterol by high-field ESR,²⁰ it was found that the nitroxide group tends to be excluded from the densely packed gel-phase bilayer, similar to the exclusion of solutes from crystallizing solvents. In this case the acyl chains are forced to take bent conformations so that the nitroxide moiety is located at the same depth for all PC in the polar part of the bilayer. Consistent with this conclusion, Figure 13 shows

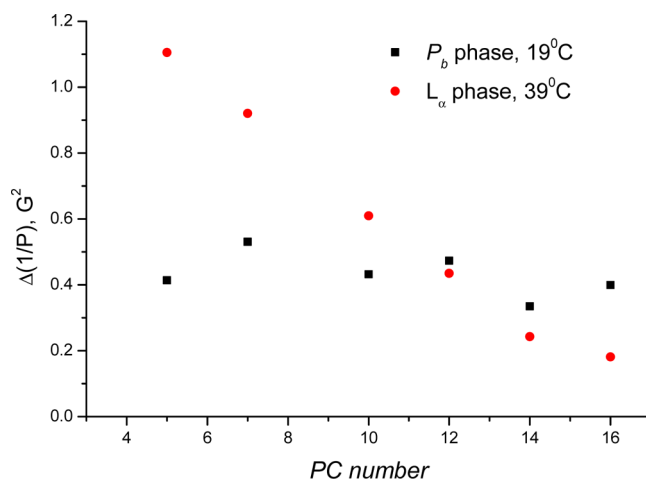


Figure 13. Relaxation enhancement from 10 mM of Ni(ClO₄)₂ introduced into the water phase of lipid DMPC dispersions as a function of n at the P_β (19 °C) and L_α (39 °C).

the dependence of the RE parameter $\Delta(1/P)$ by 10 mM of Ni(ClO₄)₂ on the spin-labeling position for the gel phase in comparison to liquid crystal phase of DMPC. In the liquid crystal phase ($T = 39$ °C) the interaction with the paramagnetic relaxant decreases with increasing n , consistent with an increase in the average immersion depth of the spin-label moiety in the membrane (see below). On the contrary, the $\Delta(1/P)$ profile in the gel phase (P_β, $T = 19$ °C) is nearly flat. These results from the gel phase highlight the acyl chains' flexibility and imply a possible role of acyl chain bending in the liquid crystal phase as well.

DISCUSSION

In this section we discuss the nature of the magnetic interaction between the membrane-embedded nitroxides of PC spin-labels and paramagnetic metal ions located in the water phase. We show there is overwhelming evidence that this interaction with

Ni²⁺ occurs via Heisenberg exchange (HE). We suggest that the close ion-nitroxide contact required for this HE occurs at the membrane surface to which nitroxides of all PC spin-labels can reach due to conformational fluctuations of the acyl chain. We demonstrate that this model is consistent with the experimental observations, e.g., very gradual dependence of RE on the PC number. Also, using different ions of d- and f-shell elements, we show that Heisenberg exchange and two different types of dipole–dipole interactions, namely static and dynamic, are manifested in the membrane environment.

1. How Do Ions and Lipid Spin-Labels Interact? Spin-Dependent Mechanisms of the Relaxation Enhancement for Different Paramagnetic Ion. We discussed in the Results section a variety of factors that affect the RE for the membrane-embedded PC labels by paramagnetic cations present in the aqueous phase. These factors include the nature and concentration of the relaxant cation, counterion, other electrolytes present in the water phase, membrane composition, etc. Now we discuss the electron-spin-dependent mechanisms of the observed RE for different paramagnetic cations. There are two possible mechanisms of magnetic interaction between nitroxide labels in the lipid phase and paramagnetic ions at the membrane surface. We note that dipole–dipole (D–D) interactions between the spin probe and the paramagnetic ion are generally dominant in solids, whereas Heisenberg exchange (HE) prevails in nonviscous liquids.^{47,48} A good example of these two competing mechanisms vs temperature in phospholipid membranes with a detailed discussion of their relative contributions depending on the complex diffusion processes in the bilayer is given in ref 49. (See also the detailed analysis of T_2 dependence on the rate of molecular diffusion due to D–D interactions by Nevzorov–Freed given in refs 50 and 51.)

If we assume that nitroxides of n -PC spin-labels are predominantly in an all-trans conformation and located for $n > 9$ in the hydrophobic core of the membrane, then there would be no opportunity for HE and D–D interactions would be dominant.

However, estimates for D–D interactions give for Ni²⁺ ions extremely low values of RE compared to experimental observations.¹⁹ Moreover, the estimates should be considered an upper limit because they do not include partial motional averaging in the fluid membrane. We will discuss this matter further below (section HE vs D–D).

Kulikov and Lichtenstein²⁶ have adapted the Solomon–Bloembergen equations^{52,53} for the case of D–D relaxation of the nitroxide dominated by the rapidly relaxing metal ion and did not include motional effects. According to their treatment

$$\frac{1}{T_{1,dd,static}^{(i)}} = \frac{|\mu_R|^2 \gamma_e^2}{6r_i^6} \left\{ (1 - 3 \cos^2 \Omega_i)^2 \times \frac{\tau_{2,R}}{1 + (\omega_L - \omega_R)^2 \tau_{2,R}^2} + \frac{9}{2} \sin^2 2\Omega_i \times \frac{\tau_{1,R}}{1 + \omega_L^2 \tau_{1,R}^2} + \frac{9}{2} \sin^4 \Omega_i \times \frac{\tau_{2,R}}{1 + (\omega_L + \omega_R)^2 \tau_{2,R}^2} \right\} \quad (5)$$

$$\frac{1}{T_{2,dd,static}^{(i)}} = \frac{|\mu_R|^2 \gamma_e^2}{6r_i^6} \left\{ 2(1 - 3 \cos^2 \Omega_i)^2 \tau_{1,R} + \frac{9}{2} \sin^2 2\Omega_i \times \frac{\tau_{2,R}}{1 + \omega_R^2 \tau_{1,R}^2} + \frac{(1 - 3 \cos^2 \Omega_i)^2}{2} \times \frac{\tau_{2,R}}{1 + (\omega_L - \omega_R)^2 \tau_{2,R}^2} + \frac{9}{4} \times \sin^2 2\Omega_i \times \frac{\tau_{1,R}}{1 + \omega_L^2 \tau_{1,R}^2} + \frac{9}{2} \times \sin^4 \Omega_i \times \frac{\tau_{2,R}}{1 + (\omega_L + \omega_R)^2 \tau_{2,R}^2} \right\} \quad (6)$$

where ω_R and ω_L are the Larmor frequencies of the paramagnetic ion and spin-label, r_i is the distance between the paramagnetic ion and spin-label, Ω_i is the angle between the interdipolar vector \mathbf{r}_i and the magnetic field direction, $\tau_{1,R}$ and $\tau_{2,R}$ are the paramagnetic relaxation times of the paramagnetic ion, and μ_R is its magnetic moment. For Ni, for example, $\tau_{1,R} = \tau_{2,R}$. (We will discuss below limitations⁵⁴ on the applicability of these equations.)

It has been shown¹⁹ that for paramagnetic ions adsorbed at the lipid–water interface of lipid vesicles with random orientation of the membrane normal relative to the magnetic field direction eqs 5 and 6 can be substantially simplified by integration over paramagnetic ion distribution. It yields for the case of $\tau_{1,R} = \tau_{2,R}$:

$$\frac{1}{T_{1,dd(static)}^{(i)}} = \frac{\pi \mu_R^2 \gamma_e^2}{45 R^4} \tau_{1,R} c f_1(\omega_L, \omega_R) \quad (7)$$

$$\frac{1}{T_{2,dd(static)}^{(i)}} = \frac{\pi \mu_R^2 \gamma_e^2}{30 R^4} \tau_{1,R} c f_2(\omega_L, \omega_R) \quad (8)$$

where

$$f_1(\omega_L, \omega_R) = \frac{1}{1 + (\omega_L - \omega_R)^2 \tau_{1,R}^2} + \frac{3}{1 + \omega_L^2 \tau_{1,R}^2} + \frac{6}{1 + (\omega_L + \omega_R)^2 \tau_{1,R}^2}$$

and

$$f_2(\omega_L, \omega_R) = 4 + \frac{1}{1 + (\omega_L - \omega_R)^2 \tau_{1,R}^2} + \frac{3}{1 + \omega_L^2 \tau_{1,R}^2} + \frac{6}{1 + \omega_R^2 \tau_{1,R}^2} + \frac{6}{1 + (\omega_L + \omega_R)^2 \tau_{1,R}^2}$$

We take the RE to be in general proportional to $S(S+1) \times \tau_{1,R}$, where S is the electron spin of the ion, $\tau_{1,R}$ is its relaxation time, and $f_2(\omega_L, \omega_R)$ is ~ 4 for Cu, Mn, and Gd and ~ 20 for Ni, Co, and Dy.¹⁹ A comparison of different paramagnetic ions having different electron paramagnetic dipolar moments and relaxation times gives the following SB equation estimates relative to Ni = 1 for dipole RE at the same surface concentration for different ions: Gd³⁺ ~ 250 , Mn²⁺ ~ 2500 , Cu²⁺ ~ 80 , Co²⁺ ~ 0.08 , and Dy³⁺ ~ 2.5 .

On the basis of these estimates, one would expect nearly 2 orders of magnitude larger RE from D–D interactions for Gd^{3+} over Ni^{2+} for the same concentrations of both ions at the membrane surface. Indeed, as follows from Results, subsection 5, the surface concentrations of Gd^{3+} and Ni^{2+} at the conditions of our saturation experiments are similar. Instead, as one can see from Figure 17, the RE effect of these two ions is similar as discussed in subsection 3. Also, according to estimates based on eqs 7 and 8, Dy^{3+} ion should show a larger effect than Ni^{2+} , whereas experiments in membranes give for nickel about an order of magnitude larger RE than for Dy^{3+} .

While estimates based on the $S(S+1) \times \tau_{1,R}$ values do not yield good estimates for the fluid phase membrane environment, in frozen water–glycerol glasses at 120 K they give a relatively good prediction for the order of observed relaxation effects (cf. Supporting Information, subsection 3) if one takes into account the $\tau_{1,R}$ values of the ions at this low temperature. At such conditions relaxation enhancement of Tempo, as $\Delta(1/P)$, is 0.0012 G^2 at a 10 mM concentration of NiCl_2 or $\text{Ni}(\text{ClO}_4)_2$ and 0.06 G^2 at 50 mM, which makes nickel a very weak dipolar relaxation enhancer compared to most other ions. These concentrations of ions correspond to average separations between them of 55 and 32 Å respectively, and the separation of ~ 40 Å between ions at the DMPC surface for 10 mM $\text{Ni}(\text{ClO}_4)_2$ is well within this range. However, in membranes at 39 °C $\Delta(1/P)$ values are nearly 2 orders of magnitude larger than in a frozen glass, despite an expectation of a decrease in the magnitude of D–D interactions with increase in temperature due to their motional averaging and the faster relaxation of the Ni ion. All this suggests a different mechanism of interaction between nitroxides of PC spin-labels and nickel ions.

Remarkably, RE values for PC labels by different ions in membranes correlate reasonably well with the broadening effects of these ions in homogeneous solutions of nitroxides, where there are direct collisions between ions and radicals, see Table 1 and Figure 14.

Table 1. Effective Heisenberg Exchange Constants in Units of $\text{M}^{-1} \text{ s}^{-1}$ Determined from Broadening of Corresponding Nitroxide Lines by Metal Salts in Water (current study) or Methanol (ref 19)

$\text{CuSO}_4/\text{tempo}/\text{water}$	9.4×10^8	$\text{CuCl}_2/10\text{PC}/\text{methanol}$	1.8×10^9
$\text{NiSO}_4/\text{tempo}/\text{water}$	5.9×10^8	$\text{NiCl}_2/10\text{PC}/\text{methanol}$	1.1×10^9
$\text{CoCl}_2/\text{tempo}/\text{water}$	6.1×10^7	$\text{CoCl}_2/10\text{PC}/\text{methanol}$	1.3×10^8
$\text{DyCl}_3/\text{tempo}/\text{water}$	5.3×10^7	$\text{DyCl}_3/10\text{PC}/\text{methanol}$	5×10^7

Further indication of direct contact yielding Heisenberg exchange between PC labels and nickel ions is given by a comparison of PC labels with DPPTC, which is a headgroup labeled lipid. If we assume that PC labels in the bilayer never reach the water phase (or near-water region), one should expect a large difference in RE induced by water-soluble nickel salts on spin-labels exposed to the water phase vs spin located inside of the lipid bilayer. The nitroxide moiety of DPPTC is attached to the charged choline group and most time stays at the membrane interface. It should be accessible to compounds dissolved in the water phase or adsorbed at the interface. However, the broadening caused by $\text{Ni}(\text{ClO}_4)_2$ is very similar for DPPTC and 5-PC, and it maintains the same order of magnitude even as it decreases for other PC spin-labels (Figure 15). This is consistent with HE.

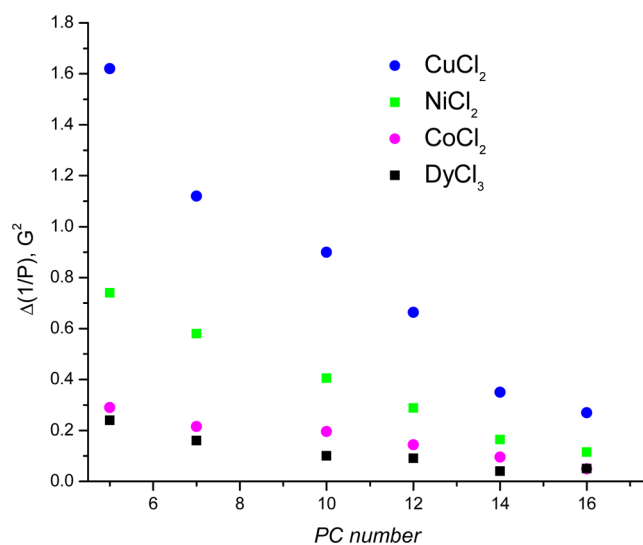


Figure 14. Comparative effect of metal ions on relaxation of *n*-PC spin-labels in the DMPC membrane. The salt concentration is 30 mM.

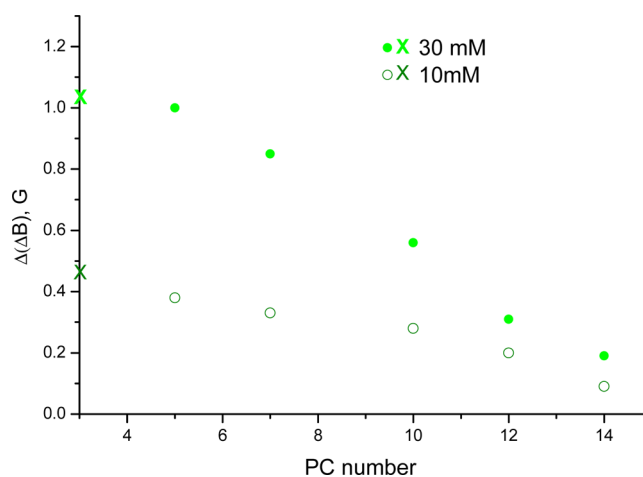


Figure 15. Effect of 30 and 10 mM of $\text{Ni}(\text{ClO}_4)_2$ on the line width of different PC spin-labels (circles) and DPPTC (crosses).

Direct contact required for HE between the doxyl group bound to the acyl chain and the paramagnetic relaxant can occur either by penetration of the relaxant into the membrane, as observed for oxygen for example, or by bending the spin-labeled acyl chain, so that it takes on a conformation with the nitroxide at the membrane surface thereby meeting the membrane-impermeable relaxant. Our experiments demonstrate a strong involvement of the membrane surface upon the RE and no anionic effect for DMPC. On the basis of this, and also on estimates of the free energy of transfer for anions and cations into the hydrophobic core of the membrane, we rule out the partitioning of the relaxant into the membrane (Supporting Information, subsection 4).

On the other hand, the existence of rapid and large-amplitude conformational fluctuations of acyl chains with and without doxyl labels in the liquid membrane is well-known. These fluctuations and their amplitude/frequency spectra (spatial distributions) were studied earlier by Gawrish et al.^{55–58} using the nuclear Overhauser effect and are supported by studies using fluorescent probes⁵⁹ and molecular dynamics calculations.^{57,58} As a result of these fluctuations the lipid segments and small probes including covalently attached doxyl

moieties should be described by a broad spatial distribution with a finite probability to be found at the membrane surface and to spin-exchange there with Ni^{2+} ions.

By ESR the existence of bent conformation was previously found for doxyl-stearic acids in monomolecular films,⁶⁰ water/hydrocarbon emulsion particles,⁶¹ and micellar systems.⁶² Adding the NO group appears to enhance the probability of bending the acyl chain such that the nitroxide is brought up into the polar area. We have recently shown that bent conformations of PC spin-labels are predominant in some gel-phase membranes.²⁰ Most relevant to our current study of fluid membranes is the detailed study of the distribution of the doxyl groups along the membrane normal in POPC membranes for several n -PC labels by ^1H and ^{13}C NMR relaxation measurements.⁶³ Relaxation enhancements induced for these nuclei by the interaction with the doxyl groups were observed for all lipid segments in the acyl chain below the labeling position, for glycerol and α , β , γ headgroup protons with a maximum approximately at the chain position of the probe.

Summarizing this section, we conclude that the large value of RE induced by Ni^{2+} ions on the membrane-embedded nitroxide moieties of PC spin-labels cannot be explained by D–D interactions but is consistent with HE. Direct contact between these paramagnetic species required for HE can be explained by membrane fluidity and flexibility of the nitroxide tethers which results in a broad distribution in the location of the doxyl groups including the lipid headgroup area.

2. Gradual Depth Dependence of Relaxation Enhancement for Different Ni Salts. As seen from Figures 3 and 5, the dependence of RE on the labeling position n is relatively gradual and approximately follows a $1/n$ dependence. This cannot be explained by a “ruler-like” arrangement of spin-labels interacting with ions via dipole–dipole interactions over a distance which is proportional to n . As evidenced by the anionic dependence of RE discussed above and also by the observation that binding Ni ions into a chelating compound nearly completely eliminates the RE, most ions contributing to the RE are located at the membrane surface. For this case, integrating the $1/r^6$ dependence of the RE from D–D interactions for an individual ion–nitroxide pair over all ions located on an infinite plane yields a $1/r^4$ dependence,¹⁹ much steeper than an approximately $1/r$ decrease which we observe in our experiments.

On the other hand, the existence of a broad spatial distribution of doxyl groups in membrane with a probability of reaching the headgroup region yields a much more gradual dependence on n . A conclusion of a broad conformational distribution for PC labels in the membrane can be directly drawn from the experimental bar diagrams⁶³ showing NMR proton paramagnetic relaxation rates of lipid segments in POPC multilamellar vesicles in the presence of 5-PC, 10-PC, and 16-PC. Using the data on ^1H paramagnetic relaxation rates for different lipid segments that are given in ref 63 for these spin-labels, we calculated the corresponding “normalized probabilities”:

$$w_{\text{hg}} = \frac{A_{\text{hg}}}{\sum A_i} \quad (9)$$

Here A_{hg} is the induced paramagnetic relaxation rate for headgroup protons, α , β , γ divided by the sum of the paramagnetic relaxation rates over all lipid segments including

headgroup protons. The values w_{hg} for 5-PC, 10-PC, and 16-PC are given in Table 2. As seen in the table, the values w_{hg}

Table 2

n -PC	w_{hg}
5-PC	0.114
10-PC	0.083
16-PC	0.067

change gradually with the spin-label position (n) and decrease approximately by a factor of 2 on going from 5-PC to 16-PC. This is qualitatively consistent with our experimental data.

Also, a very simplified model of a random distribution for spin-labeled tether conformations (Figure 16) puts the

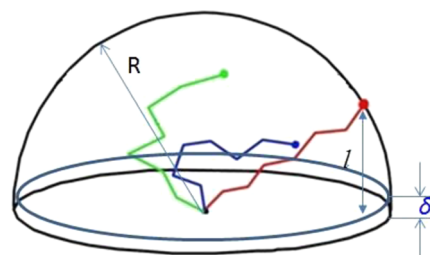


Figure 16. In the case of a random distribution of conformations for spin-labeled tethers, the nitroxide moiety can be found with equal probability in any position inside of the sphere with a radius equal to the tether length in the fully stretched conformation of the acyl chain.

nitroxide moiety in a random position inside of a half sphere with the base on the membrane surface and a radius R equal to the distance between the polar head and the nitroxide in the fully stretched conformation of the $sn2$ chain. We assume also that Heisenberg exchange between the nitroxide and the ions occurs if the nitroxide is located near the membrane surface within some $\Delta\delta$ depth. In this case the exchange frequency will be proportional to the probability of the nitroxide to be found in this layer of $\Delta\delta$ thickness. This probability will be given by a ratio of the volume of this layer, which is $\pi R^2 \Delta\delta$, to the volume of the whole hemisphere available for all possible locations of the nitroxide, $2/3 \pi R^3$. This ratio, $\pi R^2 \Delta\delta / (2/3 \pi R^3) = 3\Delta\delta / 2R$, will be inversely proportional to R and hence to n —approximately what is observed in the experiments.

Briefly summarizing this part of the discussion, we conclude that most RE observed in our experiment with Ni^{2+} salts is due to direct close contact between metal ions and nitroxide moieties of PC spin-labels. There is some evidence from molecular dynamic simulations that such contact may occur in the area of the membrane carbonyls where divalent ions adsorbed on phosphates possibly spend some time.⁶⁴

3. Heisenberg Exchange vs Dipole–Dipole Interactions. If the RE is determined primarily by the collision rate of nitroxides with the membrane surface, all RE vs n curves should have approximately the same shape for different ions and differ only in the absolute value of RE. However, as seen from Figure 17, the curves for Ni^{2+} , Cu^{2+} , and Dy^{3+} are indeed similar, but Gd^{3+} and Mn^{2+} , ions with large electron paramagnetic dipole moments and relatively long relaxation times, show an even more gradual slope.

It has been shown⁶⁵ that for nitroxides in the presence of lanthanide ions Gd^{3+} and Dy^{3+} the predominant mechanism of RE, even in homogeneous solutions of low viscosity, is dipolar.

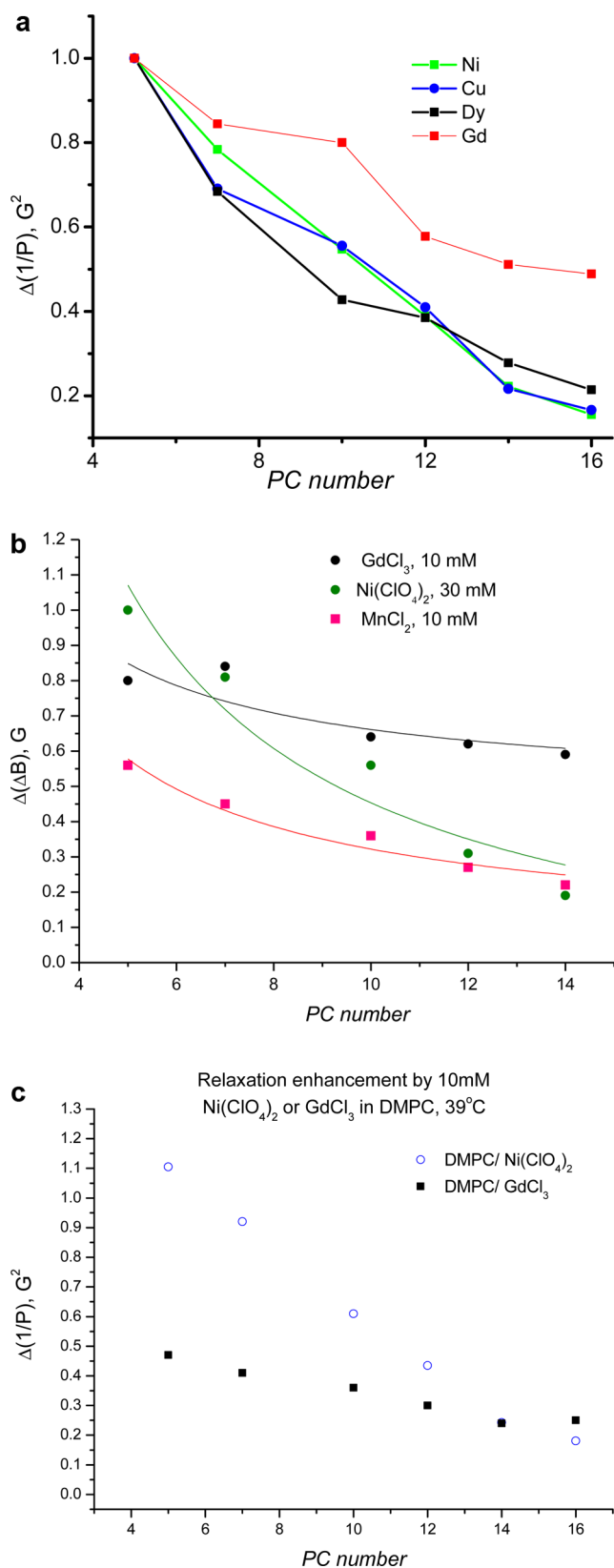


Figure 17. (a) Comparison of $\Delta(1/P)$ – n dependences for different ions for n -PC/DMPC at 39 °C. The absolute values of RE are normalized by 1 for 5-PC. One can see less steep slope of the curve for Gd. (b) Broadening of n -PC spin-labels in DMPC by 30 mM Ni(ClO₄)₂ vs 10 mM GdCl₃ and 10 mM MnCl₂. (c) RE determined in saturation experiment for 10 mM GdCl₃ and 10 mM Ni(ClO₄)₂ as $\Delta(1/P)$.

These ions have large values of electron magnetic dipolar moment but display weak exchange rates because their unpaired electrons are occupying the inner 4f shell, which is well shielded by electrons of the 5s and 5p outer shells.

This decrease in the slope can be explained by a contribution of dipole–dipole interactions in the RE induced by these ions and different mechanisms of these interactions for ions with different relaxation times (e.g., Gd³⁺ and Mn²⁺ vs Dy³⁺).

Now assume the same random distribution of conformations for the $sn2$ chain that is shown in Figure 16 with ions located at the membrane surface, but some long-distance interaction $f(r)$ (e.g., dipole–dipole mechanism) between metal ions and nitroxides. Although this interaction decreases with the immersion depth, it will be able to reach nitroxides at all conformations of the spin-labeled acyl chain, whereas Heisenberg exchange affects only conformations with nitroxides within a thin layer from the membrane surface. The relaxation enhancement from the dipole–dipole interaction averaged over all conformations of the acyl chain will be proportional to $\pi \int_0^R (R^2 - l^2) \times f(l+a) dl / 3\pi R^3$, where R is the distance between the polar group and nitroxide moiety for the fully extended conformation of n -PC, a is the distance of closest approach between nitroxides and ions with ions located at a distance of a below the base of the hemisphere, and $f(r)$ is the interaction function. The parameter a allows for avoiding infinite values of f at the membrane surface; in a physical sense it takes into account the finite ion radius and size of the nitroxide. For example, $f(r) = 1/r^3$ assuming dipole–dipole mechanism and a volume distribution of ions; $\sim 1/r^4$ results from a surface distribution.¹⁹ For Heisenberg exchange (see above) $f = \delta(r)$; it yields a hyperbolic dependence from n , while any other $f(r)$ than $\delta(r)$ will result in a somehow less steep dependence of the RE (Figure 18) on n . Note that $f = 1/r^3$ and $f = 1/r^4$ only slightly differ from the $1/n$ pattern, and it cannot be reliably detected experimentally.

However, eqs 7 and 8 describe the RE induced by paramagnetic ions on organic radicals only in the case of relatively fast T_1 relaxation of the ion. Even in this case the theory is not fully valid for slowly rotating systems when the electronic levels are split at zero field, in which case a modified

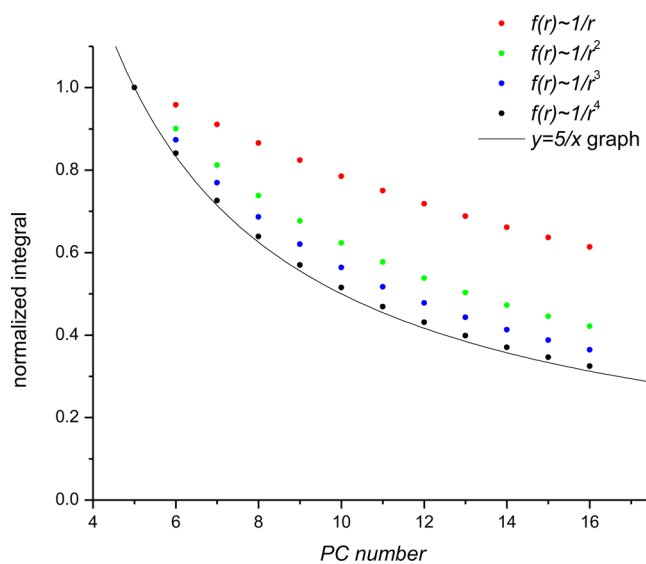


Figure 18. Dependences of the normalized integral $\pi \int_0^R (R^2 - l^2) \times f(l+a) dl / 3\pi R^3$ on the spin-labeling position n . $R = n \times$ (bond length).

theory was developed.⁵⁴ For ions with long relaxation times (e.g., Mn^{2+}) eqs 7 and 8 give a dramatic overestimate for the broadening values, since they were derived from a perturbation theory approximation, which is not valid for slow processes, e.g., slow spin–lattice relaxation. In this case the fluctuating magnetic field defining the RE emerges not from the relatively slow flip-flop of the electron spin of the ion but mainly from the mutual diffusive motion of ions and nitroxides.^{66–68} The criterion for the diffusive mechanism (dynamic, sometimes also called outer-sphere relaxation⁶⁹) prevailing over static (flip-flop of the spin) is $\tau_{\text{D}} = R^2/D$ versus $\tau_{1,\text{R}}$ where R is the interaction distance between ions and radicals; τ_{D} is sometimes called the dipolar correlation time. While for ions with short $\tau_{1,\text{R}}$ the REs induced by these ions are proportional to $\tau_{1,\text{R}}$ itself and strongly depend on the distance of minimal approach between interacting species,⁶⁶ the RE induced by mutual diffusive motion is much less sensitive to the interspin distance. Skubnevskaya and Molin⁷⁰ derived explicit formulas from ref 66 for these two limiting cases in homogeneous solutions:

$$\Delta B = \frac{32\pi}{9\sqrt{3}} N \mu^2 \gamma T_{\text{R}} \frac{1}{(a_1 + a_2)^3} \quad (\tau_{1,\text{R}} \ll \tau_{\text{D}}) \quad (10)$$

$$\Delta B = \frac{128\pi^2}{15\sqrt{3}} \frac{a_1 a_2}{(a_1 + a_2)^2} N \mu^2 \gamma \frac{\eta}{kT} \quad (\tau_{1,\text{R}} \gg \tau_{\text{D}}) \quad (11)$$

Here a_1 and a_2 are effective Stokes radii of the hydrated ion and radical, and η is the viscosity. Note that for the latter case the dependence of the RE on the interspin distance is relatively weak. For Dy^{3+} ($\tau_{1,\text{R}} \approx 3.5 \times 10^{-13} \text{ s}^{-1}$) the correlation time for D–D interactions with spin-labels in any environment is determined by $\tau_{1,\text{R}}$ alone since R is several angstroms and $D \leq 10^{-5} \text{ s}$. For Gd^{3+} τ_{D} is shorter or comparable with $\tau_{1,\text{R}}$, which is $\approx 1.4 \times 10^{-10} \text{ s}^{-1}$, from the line width of GdCl_3 in water.

The resulting RE is affected by molecular motion, at least for relatively low viscosity. The ΔB value for TEMPOL in water produced by Gd^{3+} is only ~ 12 times that for Dy^{3+} , not ~ 100 times as would follow from eq 10 and an assumption of similar distances of minimal approach between TEMPOL and either Dy^{3+} or Gd^{3+} ion. Also, eq 10 predicts larger values of dipolar broadening for Mn^{2+} vs Gd^{3+} by more than an order of magnitude while the observed line broadening by Mn^{2+} in water is only twice of that for Gd^{3+} , even though for Mn^{2+} both Heisenberg exchange and D–D contribute to the broadening.⁷⁰ Berdnikov et al.⁷¹ applied the theory outlined in ref 67 to derive a general expression for dipolar RE at any ratio of τ_{D} and τ_{R} :

$$\left(\frac{1}{T_2} \right)_{\text{dipolar}} = \frac{4\pi}{9} \frac{\gamma_i^2 \gamma_r^2 \hbar^2}{R_0^3} S(S+1) T_1 N \phi(y) \quad (12)$$

where $\phi(y) = [(4+y)y^2]/[(9+9y+4y^2+y^3)]$ and $y = (\tau_{\text{D}}/T_1)^{1/2}$; γ_i and γ_r are the gyromagnetic ratios of the ion and the radical, S is the spin of the ion, T_1 is the spin–lattice relaxation time of the ion, and N is the concentration of the paramagnetic ion. If $y \rightarrow 1$, this formula converges to relation 10. If $y \rightarrow 0$, it becomes qualitatively similar to eq 11 since $T_1 = R^2/y^2 D$ and $D \sim kT/6\pi\eta R$. This formula successfully estimates relative broadenings of nitroxides induced by Gd^{3+} or Dy^{3+} in water. For Dy^{3+} in this case $\phi(y) = 0.98$ and the formula converges to eq 10, while for Gd^{3+} $\phi(y) = 0.3$, which indicates both diffusion and T_1 of the ion contribute with the dynamic mechanism prevailing thereby substantially lowering the broadening compared to estimates based on eq 10. Another ion that

should show even stronger prevalence of the dynamic dipolar mechanism is Mn^{2+} with $\tau_{\text{R}} \approx 2.8 \times 10^{-9} \text{ s}$ (from the line width measurements) and $\phi(y) = 0.03$, but in this case the resulting broadening of nitroxide lines in solution results from both dipolar and Heisenberg exchange interactions with Mn^{2+} ions.⁷⁰

As seen from our experimental results and the above discussion, membrane fluidity and flexibility of the nitroxide tethers are the main factors explaining large values of RE for PC labels in membranes by a paramagnetic ion adsorbed at the membrane surface. However, similar to metal–nitroxide interactions in homogeneous solutions, the magnetic interaction itself may be HE, D–D, or a combination of both. The manifestations of a significant D–D contribution for Gd^{3+} and Mn^{2+} include the following:

(1) The more gradual slope of the RE- n dependence for Gd^{3+} in DMPC membranes implies a contribution of the dynamic D–D mechanism in this environment.

(2) Other indications of this mechanism for Gd^{3+} and Mn^{2+} are the absolute values of the broadening, which are much less than predicted from eq 10. Also, the relative RE ratio for Dy^{3+} , Gd^{3+} , and Mn^{2+} , which in an assumption of a “static dipole” for interactions of all three ions for the same surface concentration, should be according to eqs 7 and 8 $\sim 1:100:1000$ and in fact is $\sim 1:20:10$. Moreover, the $\sim 2:1$ ratio for Gd^{3+} vs Mn^{2+} as seen in Figure 17b approximately matches the 63/35 estimate from eq 11, the limiting case of D–D interaction with no τ_{R} effect taken into account.

(3) Also, a strong indication of the D–D mechanism, in particular the dynamic D–D interaction, is the difference between the RE values for T_1 and T_2 . Heisenberg exchange contributes equally into both T_1 and T_2 relaxation,⁴⁸ i.e., $T_{1,\text{HE}} = T_{2,\text{HE}}$, which applies for Ni^{2+} . Also, similar values of T_1 and T_2 relaxation should be observed for static D–D interactions for ions with very short $\tau_{1,\text{R}}$ as follows from eqs 7 and 8. However, as seen in comparing Figures 17b and 17c, Gd^{3+} has a weaker T_1 effect compared to its T_2 effect, since the GdCl_3 induced broadening is larger than broadening by $\text{Ni}(\text{ClO}_4)_2$, while $\Delta(1/P)$ for the same systems is larger for Ni. This requires for Gd $\Delta T_2^{-1} \geq 5\Delta T_1^{-1}$ and is consistent with a dynamic D–D interaction between Gd^{3+} and nitroxide labels if we take into account the Δg difference of 0.014 between them (Supporting Information, subsection 5).

Generally speaking, as suggested by eq 11 and Figure 17a, the dynamic D–D interaction is indeed long-range and in principle can reach the hydrophobic core from the membrane surface. Indeed, our experiments (Supporting Information, subsection 6) on spin-labeled WALP, a rigid helical peptide spanning the membrane bilayer, seem to support this suggestion, although more detailed analysis on the conformations of its spin-labeling tethers and the possibility of different alignments of the peptide in the membrane may be needed to fully interpret the results.

CONCLUSIONS

• The large values of relaxation enhancement (RE) for T_1 and T_2 for PC spin-labels in the phospholipid membrane induced by paramagnetic metal salts dissolved in the water phase can be explained by vertical fluctuations of the nitroxide group due to membrane fluidity and flexibility of lipid chains. In the case of nickel ions the predominant mechanism of RE is Heisenberg spin exchange. Other mechanisms, like longer distance dipole–dipole interactions or ion penetration into the membrane, do not contribute significantly.

- Whether the magnetic interaction occurs predominantly via Heisenberg exchange (Ni) or by dipole–dipole (Gd) interaction, getting the paramagnetic ion into close proximity with the nitroxide moiety is needed for efficient RE.

- For different salts of Ni and Cu (see also [Supporting Information](#), section S2) the RE in phosphatidylcholine membranes follows the anionic Hofmeister series and reflects adsorption of anions leading to anion-driven attraction of paramagnetic cations on the choline groups. This aspect of the adsorption is caused by the chaotropic effect and is higher for chaotropic ions, e.g., perchlorate. However, there is no anionic dependence of RE for model membranes made from negatively charged lipids (DMPG).

- This anion-driven adsorption of cations and experimental dependence of Ni-induced RE on the relaxant concentration and ionic effects can be simulated by solution of the Poisson–Boltzmann–Graham equation if one takes into account specific binding of perchlorate ions to choline groups and nickel ion to phosphates.

- In membranes with cholesterol a significant difference is observed between PC labels with nitroxide tethers long enough vs not long enough to reach deep into the membrane hydrophobic core beyond the area of fused cholesterol rings.

- Simple geometrical models taking into account flexibility of the acyl chains to which nitroxides are bound offer an explanation of the observed gradual RE dependence on the PC labeling position n .

- The dipolar mechanism of paramagnetic relaxation between nitroxides and ions, resulting from the relative diffusive motion of ions and nitroxides (Gd^{3+} , Mn^{2+}), manifests itself in an even more gradual slope of the RE vs n compared to a dominant Heisenberg exchange mechanism. This interaction is longer distance and can reach the hydrophobic core of membrane as suggested by experiments using spin-labeled WALP, a rigid helical peptide spanning the membrane bilayer ([Supporting Information](#), section S6).

- Given that the interaction of the nitroxide moiety with the paramagnetic ion either by Heisenberg exchange or by the dipole–dipole mechanism is significantly enhanced by the spin-label coming into close contact with the membrane surface, one must question the use of these magnetic interactions for probing membrane properties at different immersion depths. Those acyl chain conformations, likely of low probability, which bring the nitroxide labels close to the membrane surface necessarily make the major contributions to their spin relaxation. Although in both gel^{20–22} and fluid membrane states we observe the contributions of U-shaped conformations of nitroxide tethers, for frozen membranes these conformations are static and caused by exclusion of the bulky nitroxide from the gel phase, whereas in the fluid state studied in this work they are likely transient and short-lived.

■ ASSOCIATED CONTENT

■ Supporting Information

The Supporting Information is available free of charge on the ACS Publications website at DOI: [10.1021/acs.jpcc.5b08165](https://doi.org/10.1021/acs.jpcc.5b08165).

(S1) DSC (differential scan calorimetry) data showing the effect of metal salts on the main phase transition and pretransition in DMPC bilayers; (S2) a table showing estimates of T_1 RE for some PC labels due to several nickel and copper salts in comparison with the effect of these salts on T_2 RE; (S3) saturation curves for TEMPO

radical in frozen water/glycerol solutions containing various paramagnetic salts at 120 K; (S4) a discussion of the possibility of partition of ions or ions pairs into the membrane hydrophobic core based on thermodynamic considerations; (S5) a discussion as to how different mechanisms of RE manifest themselves by different ratios of RE for T_1 vs T_2 ; (S6) our study of RE induced by Ni^{2+} and Gd^{3+} in membrane-embedded spin-labeled WALP, a hydrophobic membrane-penetrating α -helical peptide made of alternating alanines (A) and leucines (L) flanked with tryptophans (W); (S7) estimates of diffusion rates for nitroxides yielding the viscosity in the hydrophobic core of the membrane based on our RE results ([PDF](#))

■ AUTHOR INFORMATION

Corresponding Authors

*E-mail: bd55@cornell.edu (B.D.).

*E-mail: jhf3@cornell.edu (J.F.).

Notes

The authors declare no competing financial interest.

■ ACKNOWLEDGMENTS

This work was supported by the National Institutes of Health Grants NIH/NIBIB R010EB003150 and NIH/NIGMS P41GM103521. V.L. thanks the Russian Science Foundation (grant RNF 15-13-00163) for support of his contribution to the formulation of the problem, data analysis and writing of the paper.

■ ABBREVIATIONS

ESR, electron spin resonance; DMPC, 1,2-dimyristoyl-*sn*-glycero-3-phosphocholine; DMPG, 1,2-dimyristoyl-*sn*-glycero-3-phospho-(1'-*rac*-glycerol) (sodium salt) *n*-PC spin-label-1-acyl-2-[*n*-(4,4-dimethylloxazolidine-*N*-oxyl)stearoyl]-*sn*-glycero-3-phosphocholine; DPPTC, 1,2-dipalmitoyl-*sn*-glycero-3-phospho(TEMPO)choline; TEMPO, 2,2,6,6-tetramethylpiperidine 1-oxyl; TEMPOL, 4-hydroxy-2,2,6,6-tetramethylpiperidine 1-oxyl; PD-TEMPONE, 4-oxo-2,2,6,6-tetramethylpiperidine- d_{16} -1-oxyl; CROX, potassium chromium(III) oxalate trihydrate; EDDA, ethylenediamine-*N,N'*-diacetic acid; RE, relaxation enhancement; HE, Heisenberg exchange; D–D interaction, dipole–dipole interaction.

■ REFERENCES

- (1) Finkelstein, A. Water and Non-Electrolyte Permeability of Lipid Bilayer Membranes. *J. Gen. Physiol.* **1976**, *68*, 127–135.
- (2) Subczynski, W. K.; Hyde, J. S.; Kusumi, A. Oxygen Permeability of Phosphatidylcholine-Cholesterol Membranes. *Proc. Natl. Acad. Sci. U. S. A.* **1989**, *86*, 4474–4478.
- (3) Paula, S.; Deamer, D. W. Membrane Permeability Barriers to Ionic and Polar Solutes. *Curr. Top. Membr.* **1999**, *48*, 77–95.
- (4) Mobley, H. L.; Island, M. D.; Hausinger, R. P. Molecular Biology of Microbial Ureases. *Microbiol. Rev.* **1995**, *59* (3), 451–80.
- (5) Peters, K.; Schmidt, H.; Unger, R. E.; Kamp, G.; Prols, F.; Berger, B. J.; Kirkpatrick, C. J. Paradoxical Effects of Hypoxia-Mimicking Divalent Cobalt Ions in Human Endothelial Cells in Vitro. *Mol. Cell. Biochem.* **2005**, *270* (1–2), 157–166.
- (6) Cevc, G.; Marsh, D. *Phospholipid Bilayers. Physical Principles and Models*; Wiley-Interscience: New York, 1987.
- (7) Gutknecht, J. Cadmium and Thallous Ion Permeabilities through Lipid Bilayer Membranes. *Biochim. Biophys. Acta, Biomembr.* **1983**, *735*, 185–188.

- (8) Hodgkin, A. L.; Horowitz, P. The Effect of Nitrate and Other Anions on the Mechanism of Response of Single Muscle Fibers. *J. Physiol. (Oxford, U. K.)* **1960**, *153*, 404–412.
- (9) Dani, J. A.; Sanchez, J. A.; Hille, B. Lyotropic Anions. Na Channel Gating and Ca Electrode Response. *J. Gen. Physiol.* **1983**, *81*, 255–281.
- (10) Rychkov, G. Y.; Push, M.; Roberts, M. L.; Jentsch, T. J.; Bretag, A. H. Permeation and Block of the Skeletal Muscle Chloride Channel, Cic-1, by Foreign Anions. *J. Gen. Physiol.* **1998**, *111*, 653–665.
- (11) Suzuki, K.; Post, R. L. Equilibrium of Phosphointermediates of Sodium and Potassium Ion Transport Adenosine Triphosphatase. Action of Sodium Ion and Hofmeister Effect. *J. Gen. Physiol.* **1997**, *109*, 537–554.
- (12) Norbi, J. G.; Essman, M. The Effect of Ionic Strength and Specific Anions on Substrate Binding and Hydrolytic Activities of Na, K-ATPase. *J. Gen. Physiol.* **1997**, *109*, 555–570.
- (13) Hofmeister, F. Zur Lehre Von Der Wirkung Der Salze. *Naunyn-Schmiedeberg's Arch. Pharmacol.* **1888**, *24*, 247–260.
- (14) Clarke, R. J.; Lüpfer, C. Influence of Anions and Cations on the Dipole Potential of Phosphatidylcholine Vesicles: A Basis for the Hofmeister Effect. *Biophys. J.* **1999**, *76*, 2614–2624.
- (15) Rydall, J. R.; Macdonald, P. M. Investigation of Anion Binding to Neutral Lipid Membranes Using Deuterium NMR. *Biochemistry* **1992**, *31*, 1092–1099.
- (16) Marsh, D.; Watts, A. Spin Labeling and Lipid-Protein Interactions in Membranes. In *Lipid-Protein Interactions*; Jost, P. C., Griffith, O. H., Eds.; Wiley-Interscience: New York, 1982; pp 53–126.
- (17) Nielsen, R. D.; Che, K.; Gelb, M. H.; Robinson, B. H. A Ruler for Determining the Position of Proteins in Membranes. *J. Am. Chem. Soc.* **2005**, *127*, 6430–6442.
- (18) Subczynski, W. K.; Hyde, J. S. The Diffusion-Concentration Product of Oxygen in Lipid Bilayers Using the Spin Label T1Method. *Biochim. Biophys. Acta, Biomembr.* **1981**, *643*, 283–291.
- (19) Livshits, V. A.; Dzikovski, B. G.; Marsh, D. Mechanism of Relaxation Enhancement of Spin Labels in Membranes by Paramagnetic Ion Salts: Dependence on 3d and 4f Ions and on the Anions. *J. Magn. Reson.* **2001**, *148*, 221–237.
- (20) Dzikovski, B. G.; Tipikin, D. S.; Freed, J. H. Conformational Distributions and Hydrogen Bonding in Gel and Frozen Lipid Bilayers: A High Frequency Spin-Label ESR Study. *J. Phys. Chem. B* **2012**, *116*, 6694–6706.
- (21) Dzikovski, B.; Freed, J. H. Spin Labels in the Gel Phase and Frozen Lipid Bilayers: Do They Truly Manifest a Polarity Gradient? In *Nitroxides – Theory, Experiment and Applications*; Kokorin, A. I., Ed.; InTech: Rijeka, 2012; Chapter 5, pp 167–190.
- (22) Manukovsky, N.; Sanders, E.; Matalon, E.; Wolf, S. G.; Goldfarb, D. Membrane Curvature and Cholesterol Effects on Lipids Packing and Spin-Labelled Lipids Conformational Distributions. *Mol. Phys.* **2013**, *111* (18–19), 2887–2896.
- (23) Fajer, P.; Marsh, D. Microwave and Modulation Field Inhomogeneities and the Effect of Cavity Q in Saturation Transfer ESR Spectra. Dependence on Sample Size. *J. Magn. Reson.* **1982**, *49*, 212–224.
- (24) Kooser, R. G.; Volland, W. V.; Freed, J. H. ESR Relaxation Studies on Orbitally Degenerate Free Radicals. I. Benzene Anion and Tropenyl. *J. Chem. Phys.* **1969**, *50*, 5243–5257.
- (25) Poole, C. P. *Electron Spin Resonance: A Comprehensive Treatise on Experimental Techniques*, 2nd ed.; Dover Publications, Inc.: Mineola, NY, 1996; p 780.
- (26) Kulikov, A. V.; Likhtenstein, G. I. The Use of Spin Relaxation Phenomena in the Investigation of the Structure and Model and Biological Systems. *Adv. Mol. Relax. Interact. Processes* **1977**, *10*, 47–79.
- (27) Marsh, D. Progressive Saturation and Saturation Transfer EPR for Measuring Exchange Processes of Spin-Labelled Lipids and Proteins in Membranes. *Chem. Soc. Rev.* **1993**, *22*, 329–335.
- (28) Altenbach, C.; Froncisz, W.; Hemker, R.; Mchaourab, H.; Hubbell, W. L. Accessibility of Nitroxide Side Chains: Absolute Heisenberg Exchange Rates from Power Saturation EPR. *Biophys. J.* **2005**, *89*, 2103–2112.
- (29) Goldman, S. A.; Bruno, G. V.; Freed, J. H. ESR Studies of Anisotropic Rotational Reorientation and Slow Tumbling in Liquid and Frozen Media. II. Saturation and Nonsecular Effects. *J. Chem. Phys.* **1973**, *59*, 3071–3091.
- (30) Schneider, D. J.; Freed, J. H. Calculating Slow Motional Magnetic Resonance Spectra: A User's Guide. In *Spin Labeling: Theory and Applications, Biological Magnetic Resonance* 8; Berliner, L., Ed.; Plenum: New York, 1989; pp 1–76.
- (31) Budil, D. E.; Lee, S.; Saxena, S.; Freed, J. H. Non-Linear Least Squares Analysis of Slow-Motion EPR Spectra in One and Two Dimensions Using a Modified Levenberg-Marquardt Algorithm. *J. Magn. Reson., Ser. A* **1996**, *120*, 155–189.
- (32) Livshits, V. A.; Pali, T.; Marsh, D. Relaxation Time Determinations by Progressive Saturation EPR: Effects of Molecular Motion and Zeeman Modulation for Spin Labels. *J. Magn. Reson.* **1998**, *133*, 79–91.
- (33) Livshits, V. A.; Dzikovski, B. G.; Marsh, D. Anisotropic Motion Effects in CW Non-Linear EPR Spectra: Relaxation Enhancement of Lipid Spin Labels. *J. Magn. Reson.* **2003**, *162*, 429–442.
- (34) Watts, A.; Harlos, K.; Maschke, W.; Marsh, D. Control of the Structure and Fluidity of Phosphatidylglycerol Bilayers by pH Titration. *Biochim. Biophys. Acta, Biomembr.* **1978**, *510*, 63–74.
- (35) Lamy-Freund, M. T.; Riske, K. A. The Peculiar Thermo-Structural Behavior of the Anionic Lipid DMPG. *Chem. Phys. Lipids* **2003**, *122*, 19–32.
- (36) Cevc, G.; Watts, A.; Marsh, D. Non-Electrostatic Contribution to the Titration of the Ordered-Fluid Phase Transition of Phosphatidylglycerol Bilayers. *FEBS Lett.* **1980**, *120*, 267–270.
- (37) Frias, M. A.; Contis, G.; Hollmann, A.; Disalvo, E. A. Coordination Forces between Lipid Bilayers Produced by Ferric anion and Ca²⁺. *Colloids Surf., B* **2012**, *91*, 26–33.
- (38) Aveyard, R.; Hydon, D. A. *An Introduction to the Principles of Surface Chemistry*; University Press: Cambridge, 1973.
- (39) Altenbach, C.; Seelig, J. Calcium Binding to Phosphatidylcholine Bilayers as Studied by Deuterium Magnetic Resonance. Evidence for the Formation of a Calcium Complex with Two Phospholipid Molecules. *Biochemistry* **1984**, *23*, 3913–3920.
- (40) Tatulian, S. A. Binding of Alkaline-Earth Metal Cations and Some Anions to Phosphatidylcholine Liposomes. *Eur. J. Biochem.* **1987**, *170*, 413–420.
- (41) Tatulian, S. A. Effect of Lipid Phase Transition on the Binding of Anions to Dimirystoylphosphatidylcholine Liposomes. *Biochim. Biophys. Acta, Biomembr.* **1983**, *736*, 189–195.
- (42) Marsh, D. *Handbook of Lipid Bilayers*, 2nd ed.; CRC Press: Boca Raton, FL, 2013.
- (43) Knecht, V.; Klasczyk, B. Specific Binding of Chloride Ions to Lipid Vesicles and Implications at Molecular Scale. *Biophys. J.* **2013**, *104*, 818–824.
- (44) Binder, H.; Zschörnig, O. The Effect of Metal Cations on the Phase Behavior and Hydration Characteristics of Phospholipid Membranes. *Chem. Phys. Lipids* **2002**, *115*, 39–61.
- (45) McLaughlin, A.; Grathwohl, G.; McLaughlin, S. The Adsorption of Divalent Cations to Phosphatidyl Choline Lipid Membranes. *Biochim. Biophys. Acta, Biomembr.* **1978**, *513*, 338–357.
- (46) Meshkov, B. B.; Tsybyshev, V. P.; Livshits, V. A. The Interaction of Double-Charged Metal Ions with Monolayers and Bilayers of Phospholipids. *Russ. Chem. Bull.* **1998**, *47*, 2410–2414.
- (47) Smirnova, T. I.; Smirnov, A. I.; Belford, R. L.; Clarkson, R. B. Lipid Magnetic Resonance Imaging Contrast Agent Interactions: A Spin-Labeling and a Multifrequency EPR Study. *J. Am. Chem. Soc.* **1998**, *120*, 5060–5072.
- (48) Molin, Y. N.; Salikhov, K. M.; Zamarayev, K. I. In *Spin Exchange. Principles and Applications in Chemistry and Biology*; Springer Series in Chemical Physics; Toennies, J. P., Goldanski, V. I., Eds.; Springer-Verlag: Heidelberg, 1980; Vol. 8.
- (49) Shin, Y. K.; Ewert, U.; Budil, D. E.; Freed, J. H. Microscopic Vs. Macroscopic Diffusion in Model Membranes by ESR Spectral-Spatial Imaging. *Biophys. J.* **1991**, *59*, 950–957.

(50) Nevzorov, A.; Freed, J. H. Spin Relaxation by Dipolar Coupling: From Motional Narrowing to the Rigid Limit. *J. Chem. Phys.* **2000**, *112*, 1413–1424.

(51) Nevzorov, A.; Freed, J. H. Dipolar Relaxation in a Many-Body System of Spins of 1/2. *J. Chem. Phys.* **2000**, *112*, 1425–1443.

(52) Solomon, I. Relaxation Processes in a System of Two Spins. *Phys. Rev.* **1955**, *99*, 559–566.

(53) Bloembergen, N. J. Proton Relaxation Times in Paramagnetic Solutions. *J. Chem. Phys.* **1957**, *27*, 572–573.

(54) Kowalewski, J.; Luchinat, C.; Nilsson, T.; Parigi, G. Nuclear Spin Relaxation in Paramagnetic Systems: Electron Spin Relaxation Effects under near-Redfield Limit Conditions and Beyond. *J. Phys. Chem. A* **2002**, *106*, 7376–7382.

(55) Huster, D.; Gawrish, K. Noesy NMR Crosspeaks between Lipid Headgroups and Hydrocarbon Chains: Spin Diffusion or Molecular Disorder? *J. Am. Chem. Soc.* **1999**, *121*, 1992–1993.

(56) Huster, D.; Arnold, K.; Gawrisch, K. Investigation of Lipid Organization in Biological Membranes by Two-Dimensional Nuclear Overhauser Enhancement Spectroscopy. *J. Phys. Chem. B* **1999**, *103*, 243–251.

(57) Feller, S.; Brown, C. A.; Nizza, D. T.; Gawrisch, K. Nuclear Overhauser Enhancement Spectroscopy. Cross-Relaxation Rates and Ethanol Distribution across Membranes. *Biophys. J.* **2002**, *82*, 1396–1404.

(58) Feller, S.; Huster, D.; Gawrisch, K. Interpretation of Noesy Cross-Relaxation Rates from Molecular Dynamics Simulations of a Lipid Bilayer. *J. Am. Chem. Soc.* **1999**, *121*, 8963–8964.

(59) Huster, D.; Müller, P.; Arnold, K.; Herrmann, A. The Distribution of Chain Attached 7-Nitrobenz-2oxa-1,3-Diazol-4-Yl (NBD) in Acidic Membranes Determined by 1H MAS NMR Spectroscopy. *Eur. Biophys. J.* **2003**, *32*, 47–54.

(60) Cadenhead, D. A.; Keller, B. M. J.; Muller-Landau, F. A Comparison of a Spin-Label and a Fluorescent Cell Membrane Probe Using Pure and Mixed Monomolecular Films. *Biochim. Biophys. Acta, Biomembr.* **1975**, *382*, 253–259.

(61) Dzikovski, B.; Livshits, V. EPR Spin Probe Study of Molecular Ordering and Dynamics in Monolayers at Oil/Water Interfaces. *Phys. Chem. Chem. Phys.* **2003**, *5*, 5271–5278.

(62) Baglioni, P.; Dei, L.; Rivara-Minten, E.; Kevan, L. Mixed Micelles of SDS/C₁₂E₆ and DTAC/C₁₂E₆, Surfactants. *J. Am. Chem. Soc.* **1993**, *115*, 4286–4290.

(63) Vogel, A.; Scheidt, H. A.; Huster, D. The Distribution of Lipid Attached Spin Probes in Bilayers: Application to Membrane Protein Topology. *Biophys. J.* **2003**, *85*, 1691–1701.

(64) Böckmann, R. A.; Grubmüller, H. Multistep Binding of Divalent Cations to Phospholipid Bilayers: A Molecular Dynamics Study. *Angew. Chem., Int. Ed.* **2004**, *43*, 1021–1024.

(65) Hyde, J. S.; Sarna, T. Magnetic Interactions between Nitroxide Free Radicals and Lanthanides or Cu²⁺ in Liquids. *J. Chem. Phys.* **1978**, *68*, 4439–4447.

(66) Abragam, A. *The Principles of Nuclear Magnetism*; Oxford University Press: Oxford, UK, 1961; p 599.

(67) Hwang, L. P.; Freed, J. H. Dynamic Effects of Pair Correlation Functions on Spin Relaxation by Translational Diffusion in Liquids. *J. Chem. Phys.* **1975**, *63*, 4017–4025.

(68) Freed, J. H. Dynamic Effects of Pair Correlation Functions on Spin Relaxation by Translational Diffusion in Liquids. II. Finite Jumps and Independent T₁ Processes. *J. Chem. Phys.* **1978**, *68*, 4034–4037.

(69) Kruk, D.; Kowalewski, J. Nuclear Spin Relaxation in Paramagnetic Systems (S ≥ 1) under Fast Rotation Conditions. *J. Magn. Reson.* **2003**, *162*, 229–240.

(70) Skubnevskaia, G. I.; Molin, Y. N. Exchange Interactions of Aqua-Complexes of Ions of the Iron Group Elements with Paramagnetic Particles in Solution. *Kinet. Katal.* **1967**, *8*, 1192–1197.

(71) Berdnikov, V. M.; Doktorov, A. B.; Makarshin, L. L. The Dipole-Dipole Broadening of the ESR Spectra of Free Radicals in the Presence of Paramagnetic Ions. *Theor. Exp. Chem.* **1981**, *16* (6), 554–559.